Title: Variation in paranasal pneumatisation between mid-late Pleistocene hominins

French title: Variation de la pneumatisation paranasale entre les hominines du Pléistocène moyen-finale

Author affiliations: Buck, L. T.[a,b,1], Stringer, C. B.[b], MacLarnon, A. M[c]. & Rae, T. C[a].

[a] Centre for Research in Evolutionary, Social and Inter-disciplinary Anthropology, Department of Life Sciences, University of Roehampton, Holybourne Avenue, London, SW15 4JD, UK.

[b]Human Origins Research Group, Department of Earth Sciences, Natural History Museum, Cromwell Road, London, SW7 5BD, UK.

[c]Department of Anthropology, Durham University, Dawson Building, South Road, Durham, DH1 3LE, UK.

[1]Present affiliation: PAVE Research Group, Department of Archaeology, University of Cambridge, Pembroke Street, Cambridge, CB2 3QG, UK.

Corresponding Author: Laura T. Buck. Address for correspondence (present address): PAVE Research Group, Department of Archaeology, University of Cambridge, Pembroke Street, Cambridge, CB2 3QG, UK. Email: lb396@cam.ac.uk. Telephone: +44 1223 335769.

Keywords: *Homo heidelbergensis*, sinuses, Neanderthal, Pleistocene, morphology, hominin.

French keywords: *Homo heidelbergensis*, sinus, Néanderthal, Pléistocène, morphologie, hominine.

Abstract

There is considerable variation in mid-late Pleistocene hominin paranasal sinuses and in some taxa distinctive craniofacial shape has been linked to sinus size. Extreme frontal sinus size has been reported in mid-Pleistocene specimens often classified as *Homo heidelbergensis* and Neanderthal sinuses are said to be distinctively large, explaining diagnostic Neanderthal facial shape. Here, sinuses in hominin fossils attributed to several mid-late Pleistocene taxa were compared to those of recent *H. sapiens*. The sinuses were investigated to clarify differences in the extent of pneumatisation within this group and the relationship between sinus size and craniofacial variation in hominins from this time period. Frontal and maxillary sinus volumes were measured from CT data and geometric morphometric methods were used to identify and analyse shape variables associated with sinus volume. Some mid-Pleistocene specimens were found to have extremely large frontal sinuses, supporting previous suggestions that this may be a diagnostic characteristic of this group. Contrary to traditional assertions, however, rather than mid-Pleistocene *Homo* or Neanderthals having large maxillary sinuses, this study shows that *H. sapiens* has distinctively small maxillary sinuses. While the causes of large sinuses in mid-Pleistocene *Homo* remains uncertain, small maxillary sinuses in *H. sapiens* most likely result from the derived craniofacial morphology that is diagnostic of our species. These conclusions build on previous studies to over-turn long-standing but unfounded theories about the pneumatic influences on Neanderthal craniofacial form, whilst opening up questions about the ecological correlates of pneumatisation in hominins.

French abstract: Il existe une variation considérable dans les sinus paranasaux des hominines du Pléistocène moyen-finale et dans certains taxons, la forme craniofaciale distinctive a été liée à la taille des sinus. La taille extrême des sinus frontaux a été rapportée dans les spécimens du moyen-Pléistocène, souvent classés comme *Homo heidelbergensis*, et

on dit que les sinus néandertaliens sont d'une taille nettement distincte, ce qui explique la forme diagnostique du Néanderthal. Ici, les sinus des fossiles hominiens attribués à plusieurs taxons du Pléistocène moyen-finale ont été comparés à ceux de *H. sapiens* récents. Les sinus ont été étudiés pour clarifier les différences dans l'étendue de la pneumatisation au sein de ce groupe et la relation entre la taille des sinus et la variation craniofaciale chez les hominines à partir de cette période. Les volumes des sinus frontaux et maxillaires ont été mesurés à partir de données tomodensitométriques et des méthodes morphométriques géométriques ont été utilisées pour identifier et analyser les variables de forme associées au volume sinusal. Certains spécimens du moyen-pléistocène se sont avérés avoir des sinus frontaux extrêmement grands, ce qui corrobore les suggestions précédentes selon lesquelles cela pourrait être une caractéristique diagnostique de ce groupe. Contrairement aux affirmations traditionnelles, cependant, plutôt que l'*Homo* du moyen Pléistocène ou le Néandertalien du ayant de grands sinus maxillaires, cette étude montre que *H. sapiens* á des sinus maxillaires distinctement petits. Alors que les causes des grands sinus dans l'*Homo* du Pléistocène moyen restent incertaines, les petits sinus maxillaires chez *H. sapiens* résultent très probablement de la morphologie craniofaciale dérivée qui est le diagnostic de notre espèce. Ces conclusions se fondent sur des études antérieures pour renverser des théories de longue date mais non fondées sur les influences pneumatiques sur la forme craniofaciale de Néandertal, tout en ouvrant des questions sur les corrélats écologiques de la pneumatisation chez les hominines.

Introduction

The paranasal sinuses are air-filled cavities between the inner and outer tables of the cranial bones, lined with mucous membrane [1]. Each is recognised by the position of its ostium, the hole through which mucous drains into the nasal cavity, and each is named for the bone it

most commonly pneumatises [2]. There are four types of sinus in hominins: frontal, maxillary, sphenoidal, and ethmoid; maxillary and sphenoidal sinuses are present in all hominoids, whilst the frontal and ethmoid sinuses are only found in hominines [3]. The frontal and maxillary sinuses are investigated here as they are those which are most often asserted to differ between hominin taxa [4]–[8].

Mid-late Pleistocene taxa show high levels of variation in craniofacial shape [9]. Here the mid-Pleistocene European and African fossils in our sample (Bodo, Broken Hill [Kabwe], Petralona, Steinheim and Ceprano) are referred to as *H. heidelbergensis*, despite disagreement in the field regarding the alpha taxonomy and indeed, the validity, of this species diagnosis [10], [11][10]–[12]. It is our intention to investigate the relationship between sinus size and craniofacial shape in these specimens, rather than to diagnose their taxonomy. Mid-Pleistocene specimens from Europe and Africa often attributed to *H. heidelbergensis* [13]–[19] are differentiated from *H. erectus* by an expanded upper cranial vault and increase in endocranial capacity, a vertical lateral nasal border, and reduced total facial prognathism [16], [17], [20]. Massive pneumatisation (hyperpneumatisiation) in some *H. heidelbergensis* specimens has been linked to their craniofacial morphology [6]. For example, comparatively reduced postorbital constriction in Petralona and anterior orientation of the upper face relative to the anterior cranial fossa in Petralona and Broken Hill have been related to extreme frontal pneumatisation [6], though the authors do not make it explicit whether the sinuses are regarded as the cause of craniofacial shape, or vice versa. Here associations between craniofacial morphology and sinus volume are explicitly investigated in these and other mid-Pleistocene hominins.

The complex of neurocranial features that diagnoses *H. neanderthalensis* includes a large, long, low cranium, expanded nuchal region with occipital bunning [5], [21] and a suprainiac fossa [22], [23]. Facial characteristics include swept-back zygomatics; a great degree of mid-facial prognathism [24]; double-arched supraorbital tori [22] and a large piriform aperture [22], [25]. Independently, these features are not unique to Neanderthals, but they are most frequent in this taxon and, in concert differentiate Neanderthal morphology from that of other taxa [26]. Neanderthal crania have long been characterised as being hyperpneumatised [5], [27], [28] and it has been asserted that these large sinuses resulted in diagnostic craniofacial shape. The large supraorbital tori of Neanderthals have been said to result from their expanded frontal sinuses [4], [29], and the 'inflated' Neanderthal mid-face, which projects and lacks a canine fossa, has been attributed to large maxillary sinuses [4]. This supposed hyperpneumatisation has been linked to the species' assumed adaptation to arctic conditions during the Pleistocene "ice ages", suggesting that the sinuses have a thermoregulatory role [4], [30]. Subsequent work, however, has demonstrated that sinus volume tends to decreases in cold temperatures [31]–[34], while quantification of sinus volume relative to facial size shows that the fossil taxon is indistinguishable from recent European *H. sapiens* [35], [36], but is substantially different from extant arctic people [37]. Research which has questioned the relative hyperpneumatisation of Neanderthals [35]–[37] has been limited by fairly small and geographically-restricted samples, both of fossils and of recent *H. sapiens*. It is important therefore to test the assumption of Neanderthal hyperpneumatisation and the relationship between Neanderthal pneumatisation and craniofacial shape with a more comprehensive sample.

H. sapiens is characterised by a globular cranial vault, increased basicranial flexion, anteroposteriorly short and orthognathic face, vertical forehead, presence of a canine fossa,

and a true chin [38]–[44]. Suggested causes for diagnostic *H. sapiens* morphology do not usually include sinus size, yet if it is indeed a key factor governing shape in its close congeners, *H. heidelbergensis* and Neanderthals, it could also be expected to play a part in shaping *H. sapiens* craniofacial shape. These three taxa have been central to theories of hominin sinus function [4], [29], [30], hyperpneumatisation has been argued for both *H. neanderthalensis* and *H. heidelbergensis* [6], [8], [16], and sinus form has been used as an explanation for Neanderthal and *H. heidelbergensis* characteristic shape [4], [6]. In the current study the differences in frontal and maxillary sinus size between *H. heidelbergensis*, *H. neanderthalensis*, and *H. sapiens* are measured and the relationship between sinus size and craniofacial shape investigated.

Based on the literature regarding hominin sinus size, it is hypothesised that there are significant differences between sinus volumes in different taxa, namely that either Neanderthals or *H. heidelbergensis* will be hyperpneumatised, and that these differences will be associated with taxonomically distinctive craniofacial shape. Hyperpneumatisation is clearly a relative term and when used in the literature it is not explained relative to what Neanderthals / *H. heidelbergensis* are thought to show expanded sinuses. For the purposes of this paper, hyperpneumatisation is defined as extreme sinus size in one taxon compared to the other two. If change in sinus volume causes craniofacial morphology to alter, one might expect the taxonomic differences in sinus volume between to be larger than those in craniofacial morphology, if the reverse is true and the taxonomic differences in craniofacial morphology are greater than those in sinus volume, this suggests that the craniofacial moprhology differences are proximal and drive sinus size as a secondary effect. The latter finding would have implications for our understanding of sinus function, or the lack thereof,

contributing to a long-standing debate over whether the sinuses are merely evolutionary spandrels [see 45 for review].

Previous discussions of pneumatisation [6], [45], [46] often assume that sinuses are a functionally and developmentally homogenous group. In fact, there is evidence that this is not necessarily the case; the number and type of sinuses are not constant between primate species and sinuses have been lost and regained independently on several occasions during the course of primate evolution [3], [47]. This may suggest a degree of functional heterogeneity, or at least modularity. Sinus modularity is also supported by Tillier's [48] observation of a lack of covariation in sinus size between sinus types within hominin individuals. In the current study, the frontal and maxillary sinuses were considered separately to assess the case for treating paranasal pneumatisation as a single phenomenon.

Materials and methods

Materials

The sample consists of clinical and microCT data of recent *H. sapiens* from populations with a wide geographic distribution (133 from 13 populations), early *H. sapiens* (7), *H. heidelbergensis* (5) and *H. neanderthalensis* (8) (Table 1). Data using the two forms of CT technology were combined in order to provide the maximum possible sample. The higher resolution of microCT data is likely to enable a more accurate segmentation and measurement of sinus volumes, yet comparison of measurements of the frontal and left maxillary sinuses of the specimen Broken Hill using medical and microCT show a relatively small difference. As measured by a single observer (LTB, [see 49]), the difference between

174 measurements of frontal and left maxillary sinus volumes using medical and microCT are
175 4.76% and 1.20% respectively, levels of error that were felt to be acceptable due to the
176 importance of obtaining as large a sample as possible. It is likely that the frontal sinuses are
177 most affected by the poorer resolution of medical CT, due to their more complex shape
178 (particularly in the *H. heidelbergensis* sample), which may be underestimated to some extent.
179 Thus, the level of error seen between the two measurements for Broken Hill is likely at the
180 upper end of that for any specimen.
181
182 In the current sample recent *H. sapiens* are defined as *H. sapiens* less than 25 ka and early *H.*
183 *sapiens* are defined as *H. sapiens* from between 150-25 ka following the rationale of Stringer
184 and Buck [44]. For some of the recent *H. sapiens* groups insufficient individuals were
185 available from one country to make a reasonable sample, thus samples from several countries
186 in the same region were combined if the climate, chronology and culture were comparable
187 ([50]; Table 1). Since all the recent *H. sapiens* are combined and the goal was to capture as
188 much as possible of global variation in recent *H. sapiens*, differences in levels of intragroup
189 variation between different recent *H. sapiens* samples should not affect the results.
190
191 No significant differences were found between early and recent *H. sapiens* sinus volumes or
192 sinus volume-associated craniofacial shape. Furthermore, the results presented below do not
193 change if early *H. sapiens* are omitted from the *H. sapiens* group. Thus, early and recent *H.*
194 *sapiens* are combined in the results presented here to sample the maximum possible
195 chronological and geographical variation in *H. sapiens* and due to the small sample sizes for
196 early *H. sapiens* in the morphological analyses. The fossils are shown separately in the graphs
197 (Figures 3 and 4) as with the other taxa for consistency and to show where the fossil
198 specimens fall in relation to their younger conspecifics.

Despite evidence for Neanderthal introgression in the genomes of recent *H. sapiens* [51]–[53], Neanderthals are treated here as a separate species from *H. sapiens*: *H. neanderthalensis*. It is not uncommon for closely related species to be able to interbreed to some extent [54], and levels of morphological difference between Neanderthals and *H. sapiens* are greater than those seen between many closely related species [55]–[57]. *H. heidelbergensis* is a disputed category, as mentioned above. In the analyses that follow, *H. heidelbergensis* is defined following Stringer [16], as an Afro-European species.

Only adult crania were used and pathological crania were avoided where possible. Where no alternatives were available (i.e., the fossil sample), pathological crania were used only if the pathology did not appear to alter the regions of interest (e.g., possible pathology affecting the parietals of the early *H. sapiens* fossil Singa). Whilst each recent *H. sapiens* sample was chosen to include both males and females, it was not possible to obtain exactly equal numbers without compromising sample size. Butaric et al. [58] have shown that, at least in recent *H. sapiens*, there is no sexual dimorphism in relative maxillary sinus volumes, but this is not known for frontal sinuses. There were generally more male data available, and some populations had no reliable sex information. The sample consisted of crania only (i.e., no postcrania) and no attempt was made to sex individuals based on cranial characteristics since these are very variable between populations and, as they are largely based on levels of robusticity, decisions about sex might bias craniofacial shape analyses. The sexes of the fossils are also mostly unknown; thus even correctly inferring the sex of the recent sample would not eliminate sex as a confounding variable.

Methods

Sinus volume was used to quantify sinus size [32], [33], [35], [36], [59], [60]. Sinuses were segmented manually from CT scans slice-by-slice by a single observer and their volumes measured in AVIZO versions 5-7 (FEI Visualization Sciences Group, Burlington, MA). A semi-automated method for sinus segmentation is now available [61], which may prove useful for future studies of a similar nature.

The volumes of both the right and left frontal sinuses were taken where possible (indeed, there is often no demarcation between the two), and the volume was recorded as the sum of both sides, or the only side present multiplied by two, in the instances where only one side was measurable (the Tabun C1 Neanderthal and one Western European recent *H. sapiens*). The left maxillary sinus was used if preserved and the right substituted where necessary, since there is very little bilateral asymmetry in maxillary sinuses [48].

Only crania with relatively well-preserved sinuses and surrounding craniofacial morphology were included in the study. For all samples, some of the delicate internal bones surrounding the sinuses were broken in many individuals, but by viewing the CT slices in all three planes (transverse, sagittal and coronal) in turn and also inspecting the resulting sinus volume rendered in 3D it was possible to reconstruct the original line of these bones in AVIZO on a slice-by-slice basis (see SI, Figure S1). Error testing (see below) suggests that this reconstruction is robust. Some fossil specimens have sediment in their sinus cavities, but a conservative approach was adopted whereby individuals were only included in the analyses if the sediment was of sufficiently different radio-density from the bone to be clearly visually distinguished from it. Fossil specimens with sinuses rendered and shown in situ are detailed in the Supplementary Information (Figure S2-4).

To test the precision of the method of measuring sinus volume, the two sinus types (frontal and maxillary) were sectioned out of the same recent *H. sapiens* cranial CT data five times with at least one day elapsing between measurements. These measurements were then compared and error was calculated as the sum of the differences between each individual measurement and their mean, divided by the number of measurements. This error is shown below (Table 2) as a percent of the mean measurement [62].

The measurement errors (Table 2) are low for each sinus. The recent *H. sapiens* cranium used was reasonably complete and may therefore be easier to measure accurately than some of the more broken specimens (a reasonably intact specimen was chosen to enable measurements of both sinuses on the same individual). However, the medial wall of the maxillary sinus was quite broken, which is reflected in the higher level of error in the volume for that sinus. This damage resulted in the need to estimate the position of the margins of the sinus for numerous slices (SI Figure S1), so the low level of error is reassuring. The scan is also a medical CT scan, so the level of resolution is not as high as for microCT data. For these reasons, it was felt that the error tests demonstrated the method to be sufficiently precise.

Sinus size has been shown to scale with craniofacial size in *H. sapiens* and other hominoids [36], [63]–[65]. Therefore, to look at non-isometric differences in volume, measurements must be standardised. Centroid size is one three-dimensional measurement, appropriate for the standardisation of a volume. A centroid size's quality, however, depends on the number and distribution of landmarks used to calculate it and using enough, reasonably spatially distributed, landmarks to obtain a good measure of centroid size on fragmentary specimens is problematic. In the current sample, if only the landmarks preserved on the entire sample were

used, centroid size could only be computed using four landmarks in the supraorbital region. This would clearly not give a good estimate of overall craniofacial size.

To test the possibility of using a simpler metric to standardise sinus volume and thus increase sample size, relative sinus volumes calculated using a centroid size (CS) based on a low number of landmarks (see SI, Table S1, Figure S5) were compared to relative sinus volumes calculated using a single linear measurement. A landmark set was devised to include the maximum possible sample with a minimum number of landmarks needed to capture the shape of the entire cranium (6). Despite the low number of landmarks, they are not all preserved in 75% of the fossils and 14% of the recent *H. sapiens*. In previous studies, a simple linear measurement of bi-frontomalare temporale breadth was used as a proxy for cranial size to standardise sinus volume [36], [37]. The use of half this measurement (glabella to right frontomalare temporale: G-FMT) holds the same information regarding facial size and enables all crania in the current sample to be included in at least one sinus volume analysis [49]. G-FMT was measured in AVIZO and Pearson's correlation tests were run between relative sinus volumes calculated using CS and using G-FMT. Comparison of frontal sinus volume standardisation with CS and with G-FMT produces a very strong, highly significant positive relationship ($r = 0.98$, $p < 0.001$). The relationship for maxillary sinus volumes, although still robust, has a smaller r value ($r = 0.71$, $p < 0.001$). This is perhaps not surprising, as the maxillary region is further from the measurement. Given the number of specimens that would have to be excluded if CS were used to measure size, however, the relationship was judged to be strong enough. It would have been possible to use different CSs for frontal and maxillary relative volumes, but this would have impaired comparisons between sinus types.

Craniofacial shape related to sinus volume was analysed using geometric morphometric methods (GMM). Preservation (particularly poor in the fossil sample) prevented the inclusion in the GMM analyses of the entire sample used to measure sinus volumes. Thus, reduced samples (Table 1) were used to analyse sinus-specific craniofacial shape and results from the sinus-specific shape analyses on the reduced samples are inferred to apply also to the wider sinus volume samples. To maximise sample sizes, different landmark sets were designed for each sinus and referred to as frontal/maxillary sinus-specific landmark sets (Table 3 & 4). Sinus-specific landmark sets were chosen to balance the requirements of capturing the shape of interest and including as many specimens as possible in the analyses. The intention was to capture the shape of the region of pneumatisation, but also its relationship to the rest of the cranium. For this reason, both landmark sets include a few key landmarks on the face and neurocranium outside the region of their specific sinus.

The frontal sinus-specific landmark set (Table 3) consisted of ten landmarks, mainly in the supraorbital region, allowing the inclusion of a sample of 110 specimens (Table 1). The maxillary sinus landmark set (Table 4) consisted of 13 landmarks, concentrating on the maxillary region, allowing the inclusion of 88 specimens (Table 1). These are low numbers of landmarks, but they capture shape differences between taxa and they allow the inclusion of many otherwise unusable fossils [see also 84]. Landmarks were digitised on virtual reconstructions of crania created from CT data in AVIZO. The coordinates were exported for use in Morphologika [67] and PAST [68] software. Only one half of the cranium was digitised to remove noise from individual asymmetry. The left side was digitised where there was no difference in preservation; the right was substituted if it was better preserved and mirrored in Morphologika, this allowed larger fossil sample sizes to be included.

In Morphologika, general Procrustes analyses were performed to superimpose sinus-specific landmark coordinate data for each analysis, and then Principal Components Analyses (PCA) were run. The first seven principal components (PCs), accounting for ≥70% of variance, were tested for correlations with the relevant relative sinus volumes from the wider sinus volume sample. The 70% variance cut-off point was based on the visualisation of scree-plots and scrutiny of the eigenvalues. Pearson's correlation tests, rather than regression analyses, were used to test for relationships between shape and relative sinus volume to avoid making assumptions about dependent and independent variables as one of the questions of interest is whether sinuses drive craniofacial shape or vice versa.

PC scores from each sinus-specific analysis showing significant correlation with its respective relative sinus volume [see also 35] were designated frontal or maxillary sinus volume shape parameters (the frontal SVSP and maxillary SVSP) and used in subsequent analyses (Table 5). Relative frontal sinus volume is correlated with PC6 (explaining 7% variance in shape between the sample), from the frontal sinus-specific landmark analyses this is a significant, negative correlation (r^2 = -0.12, p= < 0.001; remains significant with Bonferroni correction). Relative maxillary sinus volume is correlated with PC3 (explaining 11% of variance) from the maxillary sinus-specific landmark analysis, this is a moderate, significant positive correlation (r^2 = 0.41, p < 0.001; remains significant with Bonferroni correction).

Wireframe models (Figures 1 and 2) were created in Morphologika to visualise shape changes described by SVSPs. Frontal and maxillary SVSPs were used to determine sinus-related shape differences between taxa. Since it was not the intention of this study to study total craniofacial shape differences between individuals or groups, but to focus only on those

aspects of shape differences that are related to sinus volume, only relevant PCs with significant relationships with sinus volume (the SVSPs – Table 5) were analysed. These SVSPs were analysed individually following Zollikofer et al. [35], since this method has been shown to successfully identify relationships between sinus volume and craniofacial shape.

Given the small size of the fossil samples, the distribution of variation in their sinus volumes is unknown. The very unequal size of the samples is also likely to be problematic for parametric statistics. For these reasons, non-parametric permutation tests, ANOSIMs (analysis of similarity), were performed using PAST [68] to ascertain differences in sinus volumes and SVSP (PC) scores between taxa. An ANOSIM is analogous to an ANOVA in that it compares differences within and between groups [68]. Distances are converted to ranks and the test statistic R gives a measure of relative within group dissimilarity, with more positive numbers showing greater difference [68]. R is interpreted like a correlation coefficient and is a measure of size effect [68]. An effect size of > 0.5 is widely judged to be a large effect [69], [70], a convention followed here. Euclidean distances and 9999 permutations were used for ANOSIM analyses.

Results

Sinus volumes

There are significant differences of moderate size ($R = 0.33$, $p < 0.001$) in relative frontal sinus volumes between taxa (Figure 3). *H. heidelbergensis* has significantly larger relative frontal sinus volumes than either *H. sapiens* or *H. neanderthalensis* (Table 6).

There are large, significant differences in relative maxillary sinus volumes (Figure 3) between taxa ($R = 0.55$, $p < 0.001$). *H. sapiens* has significantly smaller relative maxillary sinus volumes than either *H. neanderthalensis* or *H. heidelbergensis* (Table 7).

Sinus-related shape

In the reduced sample analysed for frontal sinus-related shape (Table 1), the frontal SVSP showed a significant, negative correlation with frontal sinus volume ($r^2 = -0.12$, $p = < 0.001$; remains significant with Bonferroni correction). Craniofacial shapes associated with larger frontal sinuses, configurations with lower scores on the frontal SVSP (Figure 4, SI Figure S6), have relatively larger frontal and orbital regions and are taller superoinferiorly in the maxillary region (Figure 5).

There is a moderate significant difference in frontal SVSP scores (PC scores on PC6, the frontal SVSP, which explains 7% of variation) between taxonomic groups (ANOSIM: $R = 0.45$, $p < 0.005$), due to a significantly higher scores in *H. sapiens* than *H. heidelbergensis* (Figure 4, Table 8, SI Figure S4). There are no significant differences in frontal SVSP scores between Neanderthals and other taxa.

In the reduced sample analysed for maxillary sinus-related shape, the maxillary SVSP (PC3, maxillary sinus-specific landmark set, which explains 11% of variation) shows a strong, significant positive correlation with relative maxillary sinus volume ($r^2 = 0.41$, $p < 0.001$; remains significant with Bonferroni correction). Craniofacial shapes associated with relatively larger maxillary sinuses (i.e., higher scores on the maxillary SVSP – see Figure 4, SI Figure S5) have larger, taller, more anteriorly projecting faces relative to their neurocrania than craniofacial shapes associated with relatively smaller maxillary sinuses. The malar

399 region appears superoinferiorly taller in high scoring configurations and the zygomatic arch
400 appears more swept back. Higher scoring configurations also show more dolichocephalic
401 neurocrania (Figure 6).
402
403 There are differences between groups in maxillary sinus-related shape, *H. heidelbergensis*
404 falls beyond the range of variation for other taxa (Figure 4, SI Figure S5) and Neanderthals
405 fall at the upper extreme of the *H. sapiens* range of variation. This is reflected in the very
406 strong, significant difference between taxonomic groups in maxillary sinus-related shape
407 (ANOSIM: $R = 0.78$, $p < 0.001$); *H. sapiens* has significantly lower PC scores on this SVSP
408 than either *H. neanderthalensis* or *H. heidelbergensis* (see Table 9).
409
410 **Discussion**
411 Paranasal hyperpneumatisation has been discussed as a characteristic of both *H.*
412 *heidelbergensis* [6], [8], [16], [35] and *H. neanderthalensis* [4], [5], [27]–[29] and has been
413 used as an explanation for craniofacial morphology in both taxa [4], [6], [29]. Conversely,
414 recent research has suggested that compared to *H. sapiens*, *H. neanderthalensis* is not
415 hyperpneumatised when craniofacial size is taken into account [35], [36]. The aim of this
416 study was to determine the nature of pneumatic variation and its relationship to craniofacial
417 shape in mid-late Pleistocene hominins, by using the largest, most representative sample to
418 date and a more comprehensive method than previously employed. The results presented here
419 support the suggestion that frontal hyperpneumatisation is a characteristic of at least some
420 mid-Pleistocene hominins, yet refute the long-standing assertion that Neanderthals are
421 hyperpneumatised. Further, if the results from the smaller craniofacial shape sample can be
422 extended to the wider sinus volume sample, the relationship between craniofacial shape and
423 maxillary sinus volume suggests that the distinctive small, orthognathic *H. sapiens* face has

led to peculiarly small maxillary sinuses in this taxon. This may contribute to resolving long-standing arguments about sinus function [45], [46].

Frontal pneumatisation and associated craniofacial shape

The picture of *H. heidelbergensis* frontal pneumatisation from prior research is complicated, in part due to the debate over which specimens should be included in the hypodigm. Petralona, Bodo, and Broken Hill are all known for their large frontal sinuses [6], [8], [35] and similar claims have also been made for other putative *H. heidelbergensis*, such as Steinheim [8], although the current authors see little support for this latter claim based on their examination of the Steinheim CT data. Other middle Pleistocene specimens, such as Ceprano [71] and Arago 21 [48], [72]–[74], do not necessarily show the same pattern. Arago 21 is a key fossil in the *H. heidelbergensis* hypodigm, linking the mandibular (including the type specimen) and cranial material [13], [18], [20]. Although Arago 21 was unavailable for inclusion in this study, there is evidence from the literature that its frontal sinuses are small [48], [72]–[74]. They also appear to form two widely separated cells that fail to pneumatise the frontal squama [74], which is qualitatively and quantitatively different from the sinuses in Broken Hill/Bodo/Petralona, but similar those of Ceprano (Figure 7). Interestingly, Ceprano and Arago 21 are also shown to be distinctive and closely linked in other recent morphological analyses [10], distancing them from the main Euro-African *H. heidelbergensis* hypodigm (*sensu* Rightmire and Stringer [16], [20], [75], [76]), supporting a link between external craniofacial shape and frontal sinus form. Thus, from the literature it appears that, despite variation, at least a core group of middle Pleistocene *Homo* from both Europe and Africa show hyperpneumatised frontal sinuses.

448 Given the debated surrounding the taxonomic validity of *H. heidelbergensis*, it is difficult to
449 interpret the variation within the mid-Pleistocene sample. If these specimens constitute a
450 single species, the results of the current study support the assertion that the frontal sinuses of
451 *H. heidelbergensis*, relative to those of other fossil and recent hominins, are
452 hyperpneumatised. Most, but not all, of the putative *H. heidelbergensis* individuals analysed
453 have exceptional frontal pneumatisation and their overall relative frontal sinus volumes are
454 significantly greater than of the *H. sapiens* or *H. neanderthalensis* samples. Although one
455 recent *H. sapiens* has frontal pneumatisation comparable with Broken Hill, nothing in the
456 entire sample (the largest used for a similar study to date) has frontal pneumatisation
457 comparable with Bodo or Petralona. The shape and extension of the frontal sinuses of all the
458 putative *H. heidelbergensis* in this study, except Ceprano (Figure 7), appear similar and seem
459 qualitatively different from those of the other taxa in the present study and Ceprano has
460 plausibly been excluded from the *H. heidelbergensis* hypodigm based on its craniofacial
461 shape [10], [14], [41], [71], [77]. There is a high degree of variation in recent *H. sapiens*
462 sinuses [6], [78], [79] and although *H. sapiens* may be a particularly morphologically variable
463 species in general [80], we should expect at least some variation in *H. heidelbergensis*,
464 particularly given the probable temporal range for the fossil specimens in the sample [75],
465 [81]. Even taking this expected variation into account, the results from the current study
466 suggest that either *H. heidelbergensis* as a species exhibits hyperpneumatised frontals
467 compared to *H. sapiens* and *H. neanderthalensis*, or that there is a polyphyletic group of mid-
468 Pleistocene hominins from Europe and Africa who share hyperpneumatised frontal sinuses
469 through convergent evolution. The latter is perhaps a more interesting question for the
470 discussion of sinus function, as it could open interesting investigations as to which aspects of
471 ecology (if the sinuses are functional) or craniofacial shape (if the sinuses are spandrels) these
472 specimens share that could have led to hyperpneumatisation.

Both statements above assume that hyperpneumatisation is not the primitive condition, yet based on the evidence to date, this is uncertain, given the equivocal knowledge of sinus volume in *H. erectus*. The one *H. erectus* specimen available for sinus volume measurement in the current study (KNM-ER 3883, not included in statistical and shape analyses as the sole representative of its taxon) has a similar relative frontal sinus volume to Broken Hill. Taken alone, this would suggest that large frontal sinuses may be the primitive condition [82]. Where it is sufficiently preserved, however, the African *H. erectus* sample in fact suggests that small frontal sinuses restricted to the supraorbital region are the norm for *H. erectus* [83] and the majority of Asian *H. erectus* also have small frontal sinuses that do not extend superiorly past the glabellar region [48], [72], [74], [84]–[87]. Thus the general impression is of a small frontal sinus in *H. erectus*, with some exceptions such as KNM-ER 3833, quite different from the morphology of at least most *H. heidelbergensis* specimens, as shown in this study. This suggests that frontal hyperpneumatisation is derived in some mid-Pleistocene hominins.

In addition to the clear difference in relative frontal sinus volumes discussed above, inter-taxonomic differences were also found in the reduced sample analysis of frontal sinus-related craniofacial shape (*H. heidelbergensis* sample: Broken Hill and Petralona). It has been argued that hyperpneumatisation is a cause of the distinctive *H. heidelbergensis* craniofacial shape [6]. Conversely, the shape of the frontal bone [74], the orbital [35] and supraorbital regions [79] have been suggested as influences on frontal sinus form. In the reduced *H. heidelbergensis* sample specimens show significant differences in frontal sinus-related craniofacial shape from *H. sapiens*. *H. heidelbergensis* have taller supraorbital regions and deeper, taller faces compared to *H. sapiens*. *H. heidelbergensis* specimens often have

remarkably large supraorbital tori [16] and, in common with earlier *Homo*, *H. heidelbergensis* has a larger face than either *H. sapiens* or *H. neanderthalensis* [17]. The particularly small, retracted face of *H. sapiens* is more derived, compared to earlier *Homo*, than the distinctive face of *H. neanderthalensis* [88], [89]. It is likely that the analyses of frontal sinus-related craniofacial shape in the current study reflect these differences between *H. sapiens* and *H. heidelbergensis*. The lack of a difference in this variable between *H. heidelbergensis* and *H. neanderthalensis* may be caused by an insufficient number of landmarks to pick up on this relatively smaller shape difference.

The statistical difference between taxa in the frontal sinus-related shape analysis has a smaller effect size than for frontal sinus volume analysis. This could be construed as suggesting that the greater size of *H. heidelbergensis* frontal sinuses compared to *H. sapiens* is not only because of their differences in craniofacial shape [*contra* 3, 101, 107] and could even perhaps be interpreted as supporting the idea that differences in craniofacial shape between *H. heidelbergensis* and *H. sapiens* are affected by degree of frontal pneumatisation (cf. [6], [7]). However, the relatively few landmarks used in the present study could affect the quality of the shape data captured and the results may be affected by sample composition. Therefore, conclusions about the relative sizes effects in the two types of data should be made with caution pending further investigation. It seems unlikely that differences in pneumatisation lead to the differences in supraorbital form between *H. sapiens* and *H. heidelbergensis*, given that *H. neanderthalensis* and *H. erectus*, both have larger (although differently shaped) supraorbital tori than *H. sapiens*, yet show no relative difference in frontal sinus volume compared to *H. sapiens*.

Contrary to traditional theories regarding the cause of the supraorbital tori in Neanderthals [4], [29], but in accordance with more recent findings [35]–[37], *H. neanderthalensis* frontal sinuses were not found to be relatively larger than those of *H. sapiens*, and thus Neanderthal frontal sinuses are not hyperpneumatised. This is despite the much greater size and geographic range of the *H. sapiens* sample in the current study compared with previous research [37], [36], [35]. Several studies, including this one, have now shown that *H. neanderthalensis* does not have relatively larger frontal sinus volumes than *H. sapiens* and there is thus no evidence that differences between *H. sapiens* and *H. neanderthalensis* supraorbital shape are caused by large frontal sinuses [c.f. 9, 22, 105]. It seems reasonable, therefore, that this idea should be abandoned. What were asserted to be large sinuses in Neanderthals were used for many years to prop up theories that the Neanderthal face resulted from cold adaptation [4], [29], [30]. The lack of evidence for Neanderthal hyperpneumatisation thus also weakens the argument that their craniofacial shape is the result of hyperpolar adaptation [36], [90], (but see [91]).

Maxillary pneumatisation and associated craniofacial shape

In contrast to their frontal pneumatisation, *H. heidelbergensis* specimens in the current study do not show distinctively large maxillary sinuses compared to closely related species. However, *H. sapiens* do have significantly smaller relative maxillary sinus volumes than the other taxa (Figure 8). This provides novel evidence that *H. sapiens* has *hypo*pneumatised maxillary sinuses compared to its closest congeners. This is contrary to previous research, which not only suggested that *H. heidelbergensis* maxillary sinuses are distinctively large [e.g., 77], but also that maxillary hyperpneumatisation is a diagnostic feature and a cause of Neanderthal craniofacial morphology [e.g., 21].

In addition to differences between taxa in the full maxillary sinus volume sample, differences were also found in the reduced sample used in the maxillary sinus-related shape analyses between *H. sapiens* and the other taxa. Differences in maxillary sinus-related craniofacial shape coincide with some of the differences that are well-established as diagnosing *H. sapiens*: differences in neurocranium globularity, facial size and flatness [38]–[43], [92]. The strength of the shape differences resulting from these derived characteristics in *H. sapiens* is demonstrated by their identification by the present analyses, despite the relatively few landmarks used and the fact that the maxillary sinus-specific shape variable does not describe the greatest shape variation in the sample (it is PC3, explaining 11% of variance). The characteristic shape of *H. sapiens* (as described by the maxillary sinus-related shape variable) is associated with smaller maxillary sinuses. Despite the reduced sample size, the size effect of the difference between *H. sapiens* and *H. neanderthalensis*/*H. heidelbergensis* in maxillary sinus-associated shape is much larger than that of the difference in the relative maxillary sinus volumes themselves. This offers important evidence that the derived facial shape of *H. sapiens* leads to the distinctively small maxillary sinuses seen in our species. These results may also support theories suggesting the maxillary sinuses are in themselves functionless, their volume resulting from surrounding craniofacial form [33], [58], [60], [93], [94].

Conclusions

This study aimed to test the hypotheses that there are differences in sinus size between mid-late Pleistocene hominin taxa and that these differences are related to craniofacial shape. Sinus volume and sinus volume-associated craniofacial shape in mid-late Pleistocene hominins were compared to investigate variation in paranasal pneumatisation and its effect on craniofacial form. As construed in this study, *H. heidelbergensis* on average has a

hyperpneumatised frontal compared to *H. neanderthalensis* and *H. sapiens*, although it is not of homogenous size throughout the taxon as currently described. In addition to sinus volume differences, there are differences between taxa in frontal sinus-related craniofacial shapes. These differences are related to supraorbital torus and face size differences used to differentiate *H. heidelbergensis* from *H. sapiens* and *H. neanderthalensis* [42], [88], [89]. Larger taxonomic differences in frontal sinus-related shape than in volumes themselves could be argued to offer support for the assertion that hyperpneumatisation has shaped the distinctive craniofacial shape of these specimens [6], [7], but this seems implausible given the similarly sized external, but not internal, supraorbital morphology of *H. neanderthalensis* and *H. erectus*. Contrary to long-standing beliefs about frontal hyperpneumatisation in Neanderthals, Neanderthals do not have larger relative frontal sinuses than *H. sapiens*. This negates the role of the frontal sinuses in the large supraorbital tori of Neanderthals and does not support theories explaining distinctive Neanderthal craniofacial form as resulting from hyperpolar adaptation via pneumatisation.

In contrast to their enlarged frontal sinuses, the maxillary sinuses of *H. heidelbergensis* are not hyperpneumatised. Conversely, it can be said that the maxillary sinuses of *H. sapiens* are *hypo*pneumatised compared to *H. neanderthalensis/H. heidelbergensis*. The greater size effect of the difference in facial shape, compared to the difference in sinus size itself suggests this is a characteristic that can be explained partly by the distinctive craniofacial shape of our species. This finding overturns historical pneumatic explanations for Neanderthal maxillary shape, as the lack of significant difference in relative frontal sinus volumes between Neanderthals and *H. sapiens* does for Neanderthal supraorbital shape. The relationship between relative maxillary sinus volume and maxillary sinus-related craniofacial shape provides support for the hypothesised relationship between craniofacial shape and maxillary

sinus size, but suggests that it is craniofacial shape that is the driver of maxillary sinus size, rather than the converse. This may support assertions that the maxillary sinuses are functionless, but act as zones of accommodation, allowing modularity in the cranium [33], [58], [60], [93], [94]. The difference in relationship between face shape and sinus volume in frontal and maxillary sinuses within these taxa supports the assertion [48], [72] that the different individual sinuses may be modular and their size governed by different stimuli.

Acknowledgements

We would like to thank Antoine Balzeau and an anonymous reviewer for their constructive comments and the editor for help with French translation. LTB thanks the University of Roehampton, The Primate Society of Great Britain, and The Leakey Trust for funding. CBS's research is supported by the Calleva Foundation and the Human Origins Research Fund of the Natural History Museum, London. For kind permission to access specimens and help in collecting CT data all the authors thank Robert Kruszynski, Richie Abel, Farah Ahmed, Dan Sykes, Margaret Clegg, and Heather Bonney at the Natural History Museum; Janet Monge and Tom Schoenemann at the University of Pennsylvania; Phillipe Mennecier, Alain Fromment, and Antoine Balzeau at the Musée de l'Homme, Paris; Thomas Koppe at the Ernst-Morritz-Arndt University, Greifswald; Christoph Zollikofer at the University of Zurich; Amelie Vialet and Henry de Lumley at the Institut de Paléontologie Humaine, Paris; Giorgio Manzi at Universitá La Sapienza, Rome; Gerhard Weber at the University of Vienna; George Koufos at the Aristotle University of Thessaloniki; Luca Bondioli at the Museo Nazionale Preistorico Etnografico "Luigi Pigorini", Rome; and Andreas Pastoors at the Neanderthal Museum, Mettmann.

622

623 **Bibliography**

624 [1] H. G. Gray, *Gray's anatomy*. London: The Promotional Reprint Company Ltd., 1997.

625 [2] S. V. Negus, "The Function of the Paranasal Sinuses," *Arch. Otolaryngol. - Head Neck*
626 *Surg.*, vol. 66, no. 4, pp. 430–442, Oct. 1957.

627 [3] T. C. Rae, "Paranasal pneumatization in extant and fossil Cercopithecoidea.," *J. Hum.*
628 *Evol.*, vol. 54, no. 3, pp. 279–86, Mar. 2008.

629 [4] C. S. Coon, *The origin of races*. New York: Alfred A. Knopf, 1962.

630 [5] D. S. Brose and M. H. Wolpoff, "Early Upper Paleolithic man and Late Middle
631 Paleolithic tools," *Am. Anthropol.*, vol. 73, pp. 1156–1194, 1971.

632 [6] H. Seidler, D. Falk, C. Stringer, H. Wilfing, G. B. Müller, D. zur Nedden, G. W.
633 Weber, W. Reicheis, and J. L. Arsuaga, "A comparative study of stereolithographically
634 modelled skulls of Petralona and Broken Hill: implications for future studies of middle
635 Pleistocene hominid evolution.," *J. Hum. Evol.*, vol. 33, no. 6, pp. 691–703, Dec.
636 1997.

637 [7] F. Bookstein, K. Schäfer, H. Prossinger, H. Seidler, M. Fieder, C. Stringer, G. W.
638 Weber, J. L. Arsuaga, D. E. Slice, F. James Rohlf, W. Recheis, A. J. Mariam, and L. F.
639 Marcus, "Comparing frontal cranial profiles in archaic and modern homo by
640 morphometric analysis," *Anat. Rec.*, vol. 257, no. 6, pp. 217–224, 1999.

641 [8] H. Prossinger, H. Seidler, L. Wicke, D. Weaver, W. Recheis, C. Stringer, and G. B.
642 Müller, "Electronic removal of encrustations inside the Steinheim cranium reveals
643 paranasal sinus features and deformations, and provides a revised endocranial volume
644 estimate.," *Anat. Rec. B. New Anat.*, vol. 273, no. 1, pp. 132–42, Jul. 2003.

645 [9] S. E. Freidline, P. Gunz, K. Harvati, and J.-J. Hublin, "Middle Pleistocene human
646 facial morphology in an evolutionary and developmental context," *J. Hum. Evol.*, vol.

63, no. 5, pp. 723–740, Nov. 2012.

[10] A. Mounier and M. Caparros, “The phylogenetic status of Homo heidelbergensis – a cladistic study of Middle Pleistocene hominins,” *Bull. Mem. Soc. Anthropol. Paris*, vol. 27, no. 3–4, pp. 110–134, 2015.

[11] M. Roksandic, P. Radović, and J. Lindal, “Revising the hypodigm of Homo heidelbergensis: A view from the Eastern Mediterranean,” *Quat. Int.*, vol. 466, pp. 66–81, 2017.

[12] J. L. Arsuaga, I. Martínez, L. J. Arnold, A. Aranburu, A. Gracia-Téllez, W. D. Sharp, R. M. Quam, C. Falguères, A. Pantoja-Pérez, J. Bischoff, E. Poza-Rey, J. M. Parés, J. M. Carretero, M. Demuro, C. Lorenzo, N. Sala, M. Martinón-Torres, N. García, A. Alcázar de Velasco, G. Cuenca-Bescós, A. Gómez-Olivencia, D. Moreno, A. Pablos, C.-C. Shen, L. Rodríguez, A. I. Ortega, R. García, A. Bonmatí, J. M. Bermúdez de Castro, and E. Carbonell, “Neandertal roots: Cranial and chronological evidence from Sima de los Huesos.,” *Science*, vol. 344, no. 6190, pp. 1358–63, Jun. 2014.

[13] A. Mounier, F. Marchal, and S. Condemi, “Is Homo heidelbergensis a distinct species? New insight on the Mauer mandible.,” *J. Hum. Evol.*, vol. 56, no. 3, pp. 219–46, Mar. 2009.

[14] A. Mounier, S. Condemi, and G. Manzi, “The stem species of our species: a place for the archaic human cranium from Ceprano, Italy.,” *PLoS One*, vol. 6, no. 4, p. e18821, Jan. 2011.

[15] M. Friess, “Calvarial shape variation among Middle Pleistocene hominins: An application of surface scanning in palaeoanthropology,” *Comptes Rendus Palevol*, vol. 9, no. 6–7, pp. 435–443, Sep. 2010.

[16] C. Stringer, “The status of Homo heidelbergensis (Schoetensack 1908).,” *Evol. Anthropol.*, vol. 21, no. 3, pp. 101–7, May 2012.

[17] G. P. Rightmire, “Homo erectus and Middle Pleistocene hominins: brain size, skull form, and species recognition.,” *J. Hum. Evol.*, vol. 65, no. 3, pp. 223–52, Sep. 2013.

[18] L. T. Buck and C. B. Stringer, “Homo heidelbergensis.,” *Curr. Biol.*, vol. 24, no. 6, pp. R214-5, Mar. 2014.

[19] A. Profico, F. Di Vincenzo, L. Gagliardi, M. Piperno, and G. Manzi, “Filling the gap . Human cranial remains from Gombore II (Melka Kunture , Ethiopia ; ca . 850 ka) and the origin of Homo heidelbergensis,” vol. 94, pp. 1–24, 2016.

[20] G. P. Rightmire, “Homo in the middle pleistocene: Hypodigms, variation, and species recognition,” *Evol. Anthropol. Issues, News, Rev.*, vol. 17, no. 1, pp. 8–21, Feb. 2008.

[21] B. Vandersmeersch, “The origin of the Neandertals,” in *Ancestors: the hard evidence*, E. Delson, Ed. New York: Alan R. Liss, 1985, pp. 306–309.

[22] I. Tattersall and J. H. Schwartz, “The distinctiveness and systematic context of Homo neanderthalensis,” in *Neanderthals revisited: New approaches and perspectives*, K. Harvati and T. Harrison, Eds. Berlin: Springer, 2006, pp. 9–22.

[23] A. Balzeau and H. Rougier, “Is the suprainiac fossa a Neandertal autapomorphy? A complementary external and internal investigation,” *J. Hum. Evol.*, vol. 58, no. 1, pp. 1–22, 2010.

[24] E. Delson and C. Stringer, “Middle Pleistocene hominid variability and the origin of late Pleistocene humans.,” in *Ancestors: the hard evidence*, E. Delson, Ed. New York: Alan R. Liss, 1985, pp. 289–295.

[25] R. G. Klein, *The human career: human biological and cultural origins*. Chicago: University of Chicago Press, 1999.

[26] J.-J. Hublin, “Climatic changes, paleogeography and the evolution of the Neanderthals,” in *Neanderthals and modern humans in western Asia*, O. Akazawa, T., Aoki, K., Bar-Yosef, Ed. New York: Plenum Press, 1998, pp. 295–310.

[27] G. Busk, “On a very ancient human cranium from Gibraltar,” *Rep. 34th Meet. Br. Assoc. Adv. Sci.*, vol. (Bath 1864, pp. 91–92, 1865.

[28] C. C. Blake, “Climatic conditions for the last Neanderthals: herpetofaunal record of Gorham’s Cave, Gibraltar,” *J. Anthropol. Soc. London*, vol. 2, pp. cxxxix–clvii, 1864.

[29] M. H. Wolpoff, *Paleoanthropology*. New York: McGraw-Hill, 1999.

[30] S. E. Churchill, “Cold adaptation, heterochrony, and neandertals,” *Evol. Anthropol. Issues, News, Rev.*, vol. 7, no. 2, pp. 46–60, Jan. 1998.

[31] T. Koertvelyessy, “Relationships between the frontal sinus and climatic conditions: a skeletal approach to cold adaptation.,” *Am. J. Phys. Anthropol.*, vol. 37, no. 2, pp. 161–72, Sep. 1972.

[32] B. T. Shea, “Eskimo craniofacial morphology, cold stress and the maxillary sinus.,” *Am. J. Phys. Anthropol.*, vol. 47, no. 2, pp. 289–300, Sep. 1977.

[33] T. C. Rae, R. A. Hill, Y. Hamada, and T. Koppe, “Clinal variation of maxillary sinus volume in Japanese macaques (Macaca fuscata).,” *Am. J. Primatol.*, vol. 59, no. 4, pp. 153–8, Apr. 2003.

[34] T. C. Rae, U. S. Vidarsdóttir, N. Jeffery, and A. T. Steegmann, “Developmental response to cold stress in cranial morphology of Rattus: implications for the interpretation of climatic adaptation in fossil hominins.,” *Proc. R. Soc. London B*, vol. 273, no. 1601, pp. 2605–10, Oct. 2006.

[35] C. P. E. Zollikofer, M. S. Ponce De León, R. W. Schmitz, and C. B. Stringer, “New insights into mid-late Pleistocene fossil hominin paranasal sinus morphology.,” *Anat. Rec. (Hoboken).*, vol. 291, no. 11, pp. 1506–16, Nov. 2008.

[36] T. C. Rae, T. Koppe, and C. B. Stringer, “The Neanderthal face is not cold adapted.,” *J. Hum. Evol.*, vol. 60, no. 2, pp. 234–9, Feb. 2011.

[37] M. L. Noback, E. Samo, C. H. A. van Leeuwen, N. Lynnerup, and K. Harvati,

"Paranasal sinuses: A problematic proxy for climate adaptation in Neanderthals," *J. Hum. Evol.*, vol. 97, pp. 176–179, 2016.

[38] D. E. Lieberman, "Neanderthal and early modern human mobility patterns: comparing archaeological and anatomical evidence," in *Neanderthals and modern humans in western Asia*, New York: Plenum Press, 1998, pp. 263–275.

[39] D. E. Lieberman, "Speculations about the selective basis for modern human craniofacial form," *Evol. Anthropol. Issues, News, Rev.*, vol. 17, no. 1, pp. 55–68, Feb. 2008.

[40] D. E. Lieberman, B. M. McBratney, and G. Krovitz, "The evolution and development of cranial form in Homosapiens.," *Proc. Natl. Acad. Sci. U. S. A.*, vol. 99, no. 3, pp. 1134–9, Feb. 2002.

[41] C. Stringer, "Modern human origins: progress and prospects," *Philos. Trans. R. Soc. B Biol. Sci.*, vol. 357, no. 1420, pp. 563–579, Apr. 2002.

[42] C. Stringer, "Evolution: What makes a modern human.," *Nature*, vol. 485, no. 7396, pp. 33–5, May 2012.

[43] O. M. Pearson, "Statistical and biological definitions of 'anatomically modern' humans: Suggestions for a unified approach to modern morphology," *Evol. Anthropol. Issues, News, Rev.*, vol. 17, no. 1, pp. 38–48, 2008.

[44] C. B. Stringer and L. T. Buck, "Diagnosing Homo sapiens in the fossil record," *Ann. Hum. Biol.*, vol. 41, no. 4, pp. 312–322, Jun. 2014.

[45] S. Blaney, "Why paranasal sinuses?," *J. Laryngol. Otol.*, vol. 104, no. September, pp. 690–693, 1990.

[46] S. Márquez, "The paranasal sinuses: the last frontier in craniofacial biology.," *Anat. Rec. (Hoboken).*, vol. 291, no. 11, pp. 1350–61, Nov. 2008.

[47] T. C. Rae, T. Koppe, F. Spoor, B. Benefit, and M. McCrossin, "Ancestral loss of the

maxillary sinus in Old World monkeys and independent acquisition in Macaca," *Am. J. Phys. Anthropol.*, vol. 117, no. 4, pp. 293–296, 2002.

[48] A. M. Tillier, "Les sinus craniens chez les hommes actuels et fossiles: essai d'interpretation.," Univerisite de Paris VI, Paris, 1975.

[49] A. Balzeau, L. T. Buck, D. G. É, T. C. Rae, and C. B. Stringer, "The Internal Cranial Anatomy of the Middle Pleistocene Broken Hill 1 Cranium," *PaleoAnthropology*, vol. 2017, pp. 107–138, 2017.

[50] L. T. Buck, "Craniofacial morphology, adaptation and paranasal sinuses in Pleistocene hominins," 2014.

[51] R. E. Green, J. Krause, A. W. Briggs, T. Maricic, U. Stenzel, M. Kircher, N. Patterson, H. Li, W. Zhai, M. H.-Y. Fritz, N. F. Hansen, E. Y. Durand, A.-S. Malaspinas, J. D. Jensen, T. Marques-Bonet, C. Alkan, K. Prüfer, M. Meyer, H. A. Burbano, J. M. Good, R. Schultz, A. Aximu-Petri, A. Butthof, B. Höber, B. Höffner, M. Siegemund, A. Weihmann, C. Nusbaum, E. S. Lander, C. Russ, N. Novod, J. Affourtit, M. Egholm, C. Verna, P. Rudan, D. Brajkovic, Z. Kucan, I. Gusic, V. B. Doronichev, L. V Golovanova, C. Lalueza-Fox, M. de la Rasilla, J. Fortea, A. Rosas, R. W. Schmitz, P. L. F. Johnson, E. E. Eichler, D. Falush, E. Birney, J. C. Mullikin, M. Slatkin, R. Nielsen, J. Kelso, M. Lachmann, D. Reich, and S. Pääbo, "A draft sequence of the Neandertal genome.," *Science*, vol. 328, no. 5979, pp. 710–22, May 2010.

[52] F. Sánchez-Quinto, L. R. Botigué, S. Civit, C. Arenas, M. C. Avila-Arcos, C. D. Bustamante, D. Comas, and C. Lalueza-Fox, "North African populations carry the signature of admixture with Neandertals.," *PLoS One*, vol. 7, no. 10, p. e47765, Jan. 2012.

[53] K. Prüfer, F. Racimo, N. Patterson, F. Jay, S. Sankararaman, S. Sawyer, A. Heinze, G. Renaud, P. H. Sudmant, C. de Filippo, H. Li, S. Mallick, M. Dannemann, Q. Fu, M.

Kircher, M. Kuhlwilm, M. Lachmann, M. Meyer, M. Ongyerth, M. Siebauer, C. Theunert, A. Tandon, P. Moorjani, J. Pickrell, J. C. Mullikin, S. H. Vohr, R. E. Green, I. Hellmann, P. L. F. Johnson, H. Blanche, H. Cann, J. O. Kitzman, J. Shendure, E. E. Eichler, E. S. Lein, T. E. Bakken, L. V Golovanova, V. B. Doronichev, M. V Shunkov, A. P. Derevianko, B. Viola, M. Slatkin, D. Reich, J. Kelso, and S. Pääbo, "The complete genome sequence of a Neanderthal from the Altai Mountains.," *Nature*, vol. 505, no. 7481, pp. 43–9, Jan. 2014.

[54] C. J. Jolly, "Mixed signals: Reticulation in human and primate evolution," *Evol. Anthropol. Issues, News, Rev.*, vol. 18, no. 6, pp. 275–281, Nov. 2009.

[55] I. a N. Tattersall and J. H. Schwartz, "Morphplogy, Paleoantropology and Neanderthls," *Anat. Rec. Anat.)*, pp. 113–117, 1998.

[56] K. Harvati, "The Neanderthal taxonomic position: models of intra- and inter-specific craniofacial variation," *J. Hum. Evol.*, vol. 44, no. 1, pp. 107–132, Jan. 2003.

[57] K. Harvati, S. R. Frost, and K. P. McNulty, "Neanderthal taxonomy reconsidered: implications of 3D primate models of intra- and interspecific differences.," *Proc. Natl. Acad. Sci. U. S. A.*, vol. 101, no. 5, pp. 1147–52, Feb. 2004.

[58] L. N. Butaric, R. C. McCarthy, and D. C. Broadfield, "A preliminary 3D computed tomography study of the human maxillary sinus and nasal cavity.," *Am. J. Phys. Anthropol.*, vol. 143, no. 3, pp. 426–36, Nov. 2010.

[59] A. Balzeau and D. Grimaud-Hervé, "Cranial base morphology and temporal bone pneumatization in Asian Homo erectus.," *J. Hum. Evol.*, vol. 51, no. 4, pp. 350–9, 2006.

[60] L. N. Butaric and S. D. Maddux, "Morphological Covariation between the Maxillary Sinus and Midfacial Skeleton among Sub-Saharan and Circumpolar Modern Humans," *Am. J. Phys. Anthropol.*, vol. 160, no. 3, pp. 483–497, 2016.

[61] A. Profico, S. Schlager, V. Valoriani, C. Buzi, M. Melchionna, A. Veneziano, P. Raia, J. Moggi-Cecchi, and G. Manzi, “Reproducing the internal and external anatomy of fossil bones: two new automatic digital tools,” *Am. J. Phys. Anthropol.*, no. November 2017, 2018.

[62] T. D. White and P. A. Folkens, *The human bone manual*. Burlington, M. A.: Elsevier Academic Press, 2005.

[63] V. J. Lund, “The maxillary sinus in the higher primates,” *Acta Otolaryngol.*, vol. 105, pp. 163–171, 1988.

[64] T. Koppe, H. Nagai, and T. C. Rae, “Factors in the evolution of the primate paranasal sinuses.,” in *The paranasal sinuses of higher primates: development, function and evolution*, T. Koppe, H. Nagai, and K. W. Alt, Eds. Chicago: Quintessence, 1999, pp. 151–175.

[65] N. E. Holton, T. R. Yokley, and R. G. Franciscus, “Climatic adaptation and Neandertal facial evolution: a comment on Rae et al. (2011).,” *J. Hum. Evol.*, vol. 61, no. 5, pp. 624-7; author reply 628-9, Nov. 2011.

[66] L. Schroeder and R. R. Ackermann, “Evolutionary processes shaping diversity across the Homo lineage,” *J. Hum. Evol.*, vol. 111, pp. 1–17, 2017.

[67] P. O’Higgins and N. Jones, “Facial growth in Cercocebus torquatus: an application of three-dimensional geometric morphometric techniques to the study of morphological variation,” *J. Anat.*, vol. 193, no. 02, pp. 251–272, Aug. 1998.

[68] Ø. Hammer, D. Harper, and P. Ryan, “PAST-PAlaeontological STatistics, ver. 1.89,” *Univ. Oslo, Oslo*, no. 1999, pp. 1–31, 2001.

[69] J. Cohen, *Statistical power analysis for the behavioural sciences*. New York: Academic Press., 1988.

[70] J. Cohen, “A power primer,” *Psychol. Bull.*, vol. 112, pp. 155–159, 1992.

822 [71] E. Bruner and G. Manzi, “CT-based description and phyletic evaluation of the archaic
823 human calvarium from Ceprano, Italy.,” *Anat. Rec. A. Discov. Mol. Cell. Evol. Biol.*,
824 vol. 285, no. 1, pp. 643–58, 2005.
825 [72] A.-M. Tillier, “La pneumatisation du massif cranio-facial chez les hommes actuels et
826 fossiles (suite),” *Bull. Mem. Soc. Anthropol. Paris*, vol. 4, no. 3, pp. 287–316, 1977.
827 [73] C. Stringer, “The definition of Homo erectus and the existence of the species in Africa
828 and Europe,” *Cour. Forschungsunstitut Senckenb.*, vol. 69, pp. 131–144, 1984.
829 [74] A. Balzeau, “Spécificités des caractères morphologiques internes du squelette
830 céphalique chez Homo erectus,” Muséum national d’Histoire naturelle, Paris, 2005.
831 [75] C. B. Stringer, “Some further notes on the morphology and dating of the Petralona
832 hominid,” *J. Hum. Evol.*, vol. 12, no. 8, pp. 731–742, Dec. 1983.
833 [76] D. Lordkipanidze, M. S. P. De León, A. Margvelashvili, Y. Rak, G. P. Rightmire, A.
834 Vekua, and C. P. E. Zollikofer, “Biology of Early Homo,” no. October, pp. 326–332,
835 2013.
836 [77] G. Manzi, F. Mallegni, and A. Ascenzi, “A cranium for the earliest Europeans:
837 phylogenetic position of the hominid from Ceprano, Italy.,” *Proc. Natl. Acad. Sci. U.*
838 *S. A.*, vol. 98, no. 17, pp. 10011–6, Aug. 2001.
839 [78] J. C. Buckland-Wright, “A Radiographic Examination of Frontal Sinuses in Early
840 British Populations,” vol. 5, no. 3, pp. 512–517, 2015.
841 [79] C. J. Vinyard and F. H. Smith, “Morphometric relationships between the supraorbital
842 region and frontal sinus in Melanesian crania,” *Homo*, vol. 48, pp. 1–21, 1997.
843 [80] J. C. K. Wells and J. T. Stock, “The Biology of the Colonizing Ape The Biology of the
844 Colonizing Ape,” *Am. J. Phys. Anthropol.*, vol. 134, no. January, pp. 191–222, 2007.
845 [81] J. Clark, J. de Heinzelin, K. Schick, W. Hart, T. White, G. WoldeGabriel, R. Walter,
846 G. Suwa, B. Asfaw, E. Vrba, and al. et, “African Homo erectus: old radiometric ages

and young Oldowan assemblages in the Middle Awash Valley, Ethiopia," *Science (80-.).*, vol. 264, no. 5167, pp. 1907–1910, Jun. 1994.

[82] R. J. Sherwood, S. C. Ward, and A. Hill, "The taxonomic status of the Chemeron temporal (KNM-BC 1).," *J. Hum. Evol.*, vol. 42, no. 1–2, pp. 153–84, Jan. 2002.

[83] W. H. Gilbert, R. L. Holloway, D. Kubo, R. T. Kono, and G. Suwa, "Tomographic analysis of the Daka calvaria," in *Homo erectus: Pleistocene evidence from the Middle Awash, Ethiopia*, Berkeley: University of California Press, 2008, pp. 29–348.

[84] D. Weidenreich, *The skull of Sinanthropus pekinensis; a comparative study on a new primitive hominid skull*. Pehpei, Chungking: Geological Survey of China, 1943.

[85] D. Weidenreich, *Morphology of Solo Man*. New York: The American Museum of Natural History, 1951.

[86] X. Wu and F. E. Poirier, *Human evolution in China: A metric description of the fossils and a review of the sites*. Oxford: Oxford University Press, 1995.

[87] A. Vialet, G. Guipert, H. Jianing, F. Xiaobo, L. Zune, W. Youping, L. Tianyuan, M.-A. de Lumley, and H. de Lumley, "Homo erectus from the Yunxian and Nankin Chinese sites: Anthropological insights using 3D virtual imaging techniques," *Comptes Rendus Palevol*, vol. 9, no. 6–7, pp. 331–339, Sep. 2010.

[88] E. Trinkaus, "Neandertal faces were not long; modern human faces are short.," *Proc. Natl. Acad. Sci. U. S. A.*, vol. 100, no. 14, pp. 8142–5, Jul. 2003.

[89] E. Trinkaus, "Modern Human versus Neandertal Evolutionary Distinctiveness," *Curr. Anthropol.*, vol. 47, no. 4, pp. 597–620, 2006.

[90] J. R. Stewart, "Neanderthal–modern human competition? A comparison between the mammals associated with Middle and Upper Palaeolithic industries in Europe during OIS 3," *Int. J. Osteoarchaeol.*, vol. 14, no. 34, pp. 178–189, May 2004.

[91] S. Wroe, W. C. H. Parr, J. A. Ledogar, J. Bourke, S. P. Evans, L. Fiorenza, S. Benazzi,

J. Hublin, C. Stringer, O. Kullmer, M. Curry, T. C. Rae, and T. R. Yokley, “Computer simulations show that Neanderthal facial morphology represents adaptation to cold and high energy demands, but not heavy biting,” *Proc. R. Soc. B Biol. Sci.*, vol. 285, p. 20180085, 2018.

[92] C. Stringer, “The origin and evolution of Homo sapiens,” *Philos. Trans. R. Soc. B Biol. Sci.*, vol. 371, no. 1698, p. 20150237, 2016.

[93] S. D. Maddux and L. N. Butaric, “Zygomaticomaxillary Morphology and Maxillary Sinus Form and Function: How Spatial Constraints Influence Pneumatization Patterns among Modern Humans,” *Anat. Rec.*, vol. 300, no. 1, pp. 209–225, 2017.

[94] T. Ito, T. D. Nishimura, Y. Hamada, and M. Takai, “Contribution of the maxillary sinus to the modularity and variability of nasal cavity shape in Japanese macaques,” *Primates*, vol. 56, no. 1, pp. 11–19, 2014.

[95] S. C. Antón, “Natural history of Homo erectus,” *Am. J. Phys. Anthropol.*, vol. 122, no. S37, pp. 126–170, Jan. 2003.

[96] M. Street, T. Terberger, and J. Orschiedt, “A critical review of the German Paleolithic hominin record.,” *J. Hum. Evol.*, vol. 51, no. 6, pp. 551–79, Dec. 2006.

[97] C. Stringer, “The chronological and evolutionary postion of the Broken Hill cranium,” *Am. J. Phys. Anthropol.*, vol. S144, p. 287, 2011.

[98] G. Manzi, D. Magri, S. Milli, M. R. Palombo, V. Margari, V. Celiberti, M. Barbieri, M. Barbieri, R. T. Melis, M. Rubini, M. Ruffo, B. Saracino, P. C. Tzedakis, A. Zarattini, and I. Biddittu, “The new chronology of the Ceprano calvarium (Italy),” *J. Hum. Evol.*, vol. 59, no. 5, pp. 580–585, 2010.

[99] H. P. Schwarcz, A. Bietti, W. M. Buhay, M. C. Stiner, R. Grün, and A. Segrem, “On the reexamination of Grotta Guattari: Uranium-series and Electron-Spin-Resonance dates,” *Curr. Anthropol.*, vol. 32, no. 3, pp. 313–316, 1991.

[100] W. J. Rink, H. P. Schwarcz, F. H. Smith, and Radovĉić, “ESR ages for Krapina hominids.,” *Nature*, vol. 378, no. 6552, p. 24, Nov. 1995.

[101] R. Grün and C. Stringer, “Tabun revisited: revised ESR chronology and new ESR and U-series analyses of dental material from Tabun C1.,” *J. Hum. Evol.*, vol. 39, no. 6, pp. 601–612, 2000.

[102] L. T. Buck and C. B. Stringer, “A rich locality in South Kensington: the fossil hominin collection of the Natural History Museum, London,” *Geol. J.*, vol. 50, no. 3, pp. 321–337, 2015.

[103] F. McDermott, C. Stringer, R. Grün, C. T. Williams, V. K. Din, and C. J. Hawkesworth, “New Late-Pleistocene uranium–thorium and ESR dates for the Singa hominid (Sudan),” *J. Hum. Evol.*, vol. 31, no. 6, pp. 507–516, Dec. 1996.

[104] P. Pettitt, “The Neanderthal dead,” *he Anthropol. Hunters-gatherers*, vol. 1, pp. 1–19, Aug. 2002.

[105] P. Pettitt, *The Palaeolithic origins of human burial*. New York: Routledge, 2011.

[106] R. W. Schmitz, D. Serre, G. Bonani, S. Feine, F. Hillgruber, H. Krainitzki, S. Pääbo, and F. H. Smith, “The Neandertal type site revisited: interdisciplinary investigations of skeletal remains from the Neander Valley, Germany.,” *Proc. Natl. Acad. Sci. U. S. A.*, vol. 99, no. 20, pp. 13342–7, Oct. 2002.

[107] R. Grün, C. Stringer, F. McDermott, R. Nathan, N. Porat, S. Robertson, L. Taylor, G. Mortimer, S. Eggins, and M. McCulloch, “U-series and ESR analyses of bones and teeth relating to the human burials from Skhul.,” *J. Hum. Evol.*, vol. 49, no. 3, pp. 316–34, Sep. 2005.

[108] K. Douka, C. A. Bergman, R. E. M. Hedges, F. P. Wesselingh, and T. F. G. Higham, “Chronology of Ksar Akil (Lebanon) and implications for the colonization of Europe by anatomically modern humans.,” *PLoS One*, vol. 8, no. 9, p. e72931, Jan. 2013.

[109] D. Henry-Gambier, “Les fossiles de Cro-Magnon (Les Eyzies-de-Tayac, Dordogne:Nouvelles données sur leur position chronologique et leur attribution culturelle,” *Bull. Mem. Soc. Anthropol. Paris*, vol. 14, no. 1–2, pp. 89–112, 2002.

[110] C. C. Magori and M. H. Day, “Laetoli Hominid 18: an early Homo sapiens skull,” *J. Hum. Evol.*, vol. 12, no. 8, pp. 747–753, Dec. 1983.

[111] S. Mcbrearty and A. S. Brooks, “The revolution that wasn’t: a new interpretation of the origin of modern human behavior.,” *J. Hum. Evol.*, vol. 39, no. 5, pp. 453–563, Nov. 2000.

List of Tables

Table 1: Sample details. FVS: included in frontal sinus volume sample, FSS: included in frontal sinus-specific shape sample, MVS: included in maxillary sinus volume sample, MSS: included in maxillary sinus-specific shape sample. Y: included in analysis, N: not included in analysis. The sole *H. erectus* specimen, KNM-ER 3883, was not included in statistical analyses or figures, but is discussed in the Discussion with reference to the potential phylogenetic significance of sinus size in *H. heidelbergensis*. NMK: National Museum of Kenya; DAFH: Digital Archive of Fossil Hominins, University of Vienna; USL: Universitá La Sapienza, Rome; NHM: Natural History Museum, London; UV: University of Vienna; AUT: Aristotle University of Thessaloniki; MNPE: Museo Nazionale Preistorico Etnografico "Luigi Pigorini", Rome; MHP: Musée de l’Homme, Paris; UZ: University of Zurich; Ernst-Morritz-Arndt University, Greifswald.

French Table 1:

Détails de l'échantillon. FVS: inclus dans l'échantillon de volume du sinus frontal, FSS:

inclus dans l'échantillon de forme craniofaciale spécifique au sinus frontal, MVS: inclus dans l'échantillon de volume du sinus maxillaire, MSS: inclus dans l'échantillon de forme craniofaciale sinus maxillaire spécifique. Y: inclus dans l'analyse, N: non inclus dans l'analyse. Le seul spécimen de H. erectus, KNM-ER 3883, n'a pas été inclus dans les analyses statistiques ou les chiffres, mais il est discuté dans la discussion en référence à la signification phylogénétique potentielle de la taille des sinus chez *H. heidelbergensis*. NMK: National Museum of Kenya; DAFH: Digital Archive of Fossil Hominins, University of Vienna; USL: Universitá La Sapienza, Rome; NHM: Natural History Museum, London; UV: University of Vienna; AUT: Aristotle University of Thessaloniki; MNPE: Museo Nazionale Preistorico Etnografico "Luigi Pigorini", Rome; MHP: Musée de l'Homme, Paris; UZ: University of Zurich; Ernst-Morritz-Arndt University, Greifswald.

Table 2: Error test for sinus volume measurements. Results (mm^3) for five repetitions of sinus volume measurement (raw volume, not relative volume) and percentage error.

French Table 2: Test d'erreur pour les mesures de volume sinusal. Résultats (mm3) pour cinq répétitions de mesure du volume sinusal (volume brut, volume non relatif) et pourcentage d'erreur.

Table 3: Landmarks used in frontal sinus-specific landmark set analyses.

French Table 3: Repères utilisés dans les analyses des repères spécifiques aux sinus frontaux.

Table 4: Landmarks used in maxillary sinus-specific landmark set analyses.

French Table 4: Repères utilisés dans les analyses des repères spécifiques aux sinus maxillaire.

Table 5: Sinus volume shape parameters (SVSPs). PC: principal component from frontal/maxillary sinus-specific GMM landmark analysis. Bonferroni correction: remains significant if a Bonferroni correction is applied to reduce the likelihood of type II errors.

French Table 5: Paramètres de forme associé avec volume sinusal (SVSP). PC: composante principale d'analyse GMM spécifique au sinus frontal / maxillaire. Correction de Bonferroni: reste significative si une correction de Bonferroni est appliquée pour réduire la probabilité d'erreurs de type II.

Table 6: Results from an ANOSIM comparing relative frontal sinus volumes between taxa. The matrix is symmetrical; numbers above the trace are R values, numbers below the trace are p values. *: significant, $\alpha < 0.05$. **Bold**: remains significant if a Bonferroni correction is applied.

French Table 6: Résultats d'un ANOSIM comparant les volumes relatifs des sinus frontaux entre les taxons. La matrice est symétrique, les nombres au-dessus de la trace sont des valeurs de R, les nombres au-dessous de la trace sont des valeurs de p. *: significatif, $\alpha < 0{,}05$. Gras: reste significatif si une correction de Bonferroni est appliquée.

Table 7: ANOSIM of relative maxillary sinus volume differences between taxa. The matrix is symmetrical. Above the trace are R values, below the trace are p values; *: significant, $\alpha < 0.05$, **Bold**: remains significant if a Bonferroni correction is applied.

French Table 7: Résultats d'un ANOSIM comparant les volumes relatifs des sinus maxillaire entre les taxons. La matrice est symétrique, les nombres au-dessus de la trace sont des valeurs de R, les nombres au-dessous de la trace sont des valeurs de p. *: significatif, α <0,05. Gras: reste significatif si une correction de Bonferroni est appliquée.

Table 8: Results from ANOSIM of taxonomic position on the frontal SVSP. Matrix is symmetrical, numbers above trace are R values, and numbers below trace are p values. *: significant, $\alpha < 0.05$. **Bold:** remains significant if a Bonferroni correction is applied.

French Table 8: Résultats d'un ANOSIM comparant de la position taxonomique sur le SVSP frontal. La matrice est symétrique, les nombres au-dessus de la trace sont des valeurs de R, les nombres au-dessous de la trace sont des valeurs de p. *: significatif, α <0,05. Gras: reste significatif si une correction de Bonferroni est appliquée.

Table 9: Results from ANOSIM of taxonomic position on the maxillary SVSP. Matrix is symmetrical, numbers above trace are R values, and numbers below trace are p values. *: significant, $\alpha < 0.05$, **Bold:** remains significant if a Bonferroni correction is applied.

French Table 9: Résultats d'un ANOSIM comparant de la position taxonomique sur le SVSP maxillaire. La matrice est symétrique, les nombres au-dessus de la trace sont des valeurs de R, les nombres au-dessous de la trace sont des valeurs de p. *: significatif, α <0,05. Gras: reste significatif si une correction de Bonferroni est appliquée.

List of Figures

Figure 1: Landmarks and wireframe used for frontal sinus-specific landmark set. Numbered landmarks (Table 3) of the frontal sinus-specific landmark set seen in norma frontalis (left) and norma lateralis (right). Wireframe shows which landmarks are joined to illustrate shape changes in later figures. Dashed lines indicate links between landmarks that are not visible when the cranium is shown.

French Figure 1: Repères et wireframes utilisés pour des repères spécifiques aux sinus frontaux. Repères numérotés (Tableau 3) de l'ensemble de repères spécifiques au sinus frontal observés chez norma frontalis (à gauche) et norma lateralis (à droite). Wireframe montre quels points de repère sont joints pour illustrer les changements de forme dans les figures ultérieures. Les lignes pointillées indiquent les liens entre les points de repère qui ne sont pas visibles lorsque le crâne est affiché.

Figure 2: Landmarks and wireframe used for maxillary sinus-specific landmark set. Numbered landmarks (Table 4) of maxillary sinus-specific landmark seen in norma frontalis (left) and norma lateralis (right). Wireframe shows which landmarks are joined to illustrate shape changes in later figures. Dashed lines indicate links between landmarks that are not visible when the cranium is shown.

French Figure 2: Repères et wireframes utilisés pour des repères spécifiques aux sinus maxillaires. Repères numérotés (Tableau 3) de l'ensemble de repères spécifiques au sinus maxillaires observés chez norma frontalis (à gauche) et norma lateralis (à droite). Wireframe montre quels points de repère sont joints pour illustrer les changements de forme dans les

figures ultérieures. Les lignes pointillées indiquent les liens entre les points de repère qui ne sont pas visibles lorsque le crâne est affiché.

Figure 3: Variation in sinus size in full sample. Top: Relative (size-corrected) frontal sinus volume by taxon. Bottom: relative maxillary sinus volume by taxon. Red, R H.s: recent *H. sapiens*; blue, E H.s: early *H. sapiens*; green, H.n: *H. neanderthalensis*; magenta, H. h: *H. heidelbergensis*. CroM: Cro-Magnon, Sing: Singa, Mlad: Mladeč 1, Skh: Skhul, LaF: La Ferrassie, LaC: La Chapelle, Krap: Krapina, Feld: Feldhofer, Tab: Tabun C1, FQ: Forbes Quarry, LaQ: La Quina, Pet: Petralona, Bod: Bodo, Kab: Broken Hill, Cep: Ceprano. Recent and early *H. sapiens* shown separately in Figure, although pooled for analyses following rationale explained in Methods.

French Figure 3:

Variation de la taille des sinus dans l'échantillon complet. En haut: Volume relatif du sinus frontal relatif (corrigé en fonction de la taille) par taxon. En bas: volume relatif du sinus maxillaire par taxon. Rouge, R H.s: *H. sapiens* récent; bleu, EH: *H. sapiens* ancien; vert, H.n: *H. neanderthalensis*; magenta, H. h: *H. heidelbergensis*. CroM: Cro-Magnon, Sing: Singa, Mlad: Mladeč 1, Skh: Skhul, LaF: La Ferrassie, LaC: La Chapelle, Krap: Krapina, Feld: Feldhofer, Tab: Tabun C1, FQ: Carrière de Forbes, LaQ: La Quina, Pet: Petralona, Bod: Bodo, Kab: Broken Hill, Cep: Ceprano. *H. sapiens* récent et ancien montré séparément dans la figure, bien que regroupé pour les analyses suivant la justification expliquée dans les méthodes.

Figure 4: Variation in sinus-specific craniofacial shape in reduced sample (Table 1). Left: PCA showing frontal sinus-related craniofacial shape (Frontal SVSP, PC6 of the frontal sinus-specific landmark set analysis explaining 7% of variance) on x axis. Right: PCA of

maxillary sinus-related craniofacial shape (Maxillary SVSP, PC3 of the maxillary sinus-specific landmark set analyses explaining 11% of variance) on x axis. SVSPs (x axes) are shown against PC2 on y axes as this spreads the data more than PC1 and aids visualisation of group differences, PC2 is not correlated with frontal or maxillary sinus volume. Red triangles, R H.s: recent *H. sapiens*; blue diamonds, E. H.s: early *H. sapiens*; green squares, H.n: *H. neanderthalensis*; magenta circles, H.h: *H. heidelbergensis*. Recent and early *H. sapiens* shown separately in Figure, although pooled for analyses following rationale explained in Methods. For shape changes described by frontal and maxillary SVSPs, see Figures 5 and 6. Fossil names as above.

French Figure 4: Variation de la forme craniofaciale sinus-spécifique dans le échantillon réduit (Tableau 1). A gauche: PCA montrant la forme craniofaciale associé avec le sinus frontal (SVSP frontal, PC6 de l'analyse de l'ensemble des repères spécifiques du sinus frontal) sur l'axe des x. À droite: PCA de la forme craniofaciale associé avec le sinus maxillaire (Maxillary SVSP, PC3 des analyses de l'ensemble des points de repère spécifiques au sinus maxillaire) sur l'axe des x. Les SVSP (axes x) sont représentés par rapport à PC2 sur les axes y car cela répartit les données plus que PC1 et facilite la visualisation des différences de groupe, PC2 n'est pas corrélé avec le volume sinusal frontal ou maxillaire. Triangles rouges, R H.s: *H. sapiens* récent; diamants bleus, E.H.: *H. sapiens* ancien; carrés verts, H.n: *H. neanderthalensis*; cercles magenta, H.h: *H. heidelbergensis*. *H. sapiens* récent et ancien montré séparément sur la figure, bien que groupé pour des analyses suivant la justification expliquée dans les méthodes. Pour les changements de forme décrits par les SVSP frontal et maxillaire, voir les figures 5 et 6. Noms de fossiles comme ci-dessus.

Figure 5: Shape changes along frontal sinus volume shape parameter (SVSP). Wireframe (Figure 1) created in Morphologika showing shape changes in frontal sinus specific landmark configuration along the frontal SVSP. Left: mean configuration warped to lowest extreme of SVSP, right: mean configuration warped to highest extreme of SVSP (Figure 4). Top: norma frontalis, middle: norma lateralis.

French Figure 5: Les changements en forme du paramètre de forme du volume sinusal frontal (SVSP). Wireframe (Figure 1) créé dans Morphologika montrant des changements de forme dans la configuration du repère de sinus frontal spécifique dans la SVSP frontale. Gauche: configuration moyenne déformée au plus bas extrême de SVSP, à droite: configuration moyenne déformée au plus haut extrême de SVSP (Figure 4). En haut: norma frontalis, milieu: norma lateralis.

Figure 6: Shape changes along maxillary sinus volume shape parameter (SVSP). Wireframe (Figure 2) created in Morphologika showing shape changes in maxillary sinus-specific landmark configurations along the maxillary SVSP. Left: mean configuration warped to lowest extreme of SVSP, right: mean configuration warped to highest extreme of SVSP. Top: norma frontalis, middle: norma lateralis.

French Figure 6: Les changements en forme du paramètre de forme du volume sinusal maxillare (SVSP). Wireframe (Figure 2) créé dans Morphologika montrant des changements de forme dans la configuration du repère de sinus maxillaire spécifique dans la SVSP maxillaire. Gauche: configuration moyenne déformée au plus bas extrême de SVSP, à droite: configuration moyenne déformée au plus haut extrême de SVSP (Figure 4). En haut: norma frontalis, milieu: norma lateralis.

Figure 7: Frontal sinuses in the *H. heidelbergensis* sample. Images of the virtually reconstructed crania rendered transparent with frontal sinuses sectioned out and rendered in black. Crania scaled to approximately the same size in order to show relative size of frontal sinuses to crania, scale bars under crania = 1cm. Detail of qualitatively different Ceprano frontal sinus inset, shown from aspectus superialis. With the exception of Ceprano, all four specimens' frontal sinuses are single and continuous.

French Figure 7: Les sinus frontaux dans l'échantillon de *H. heidelbergensis*. Images de la crane reconstituée rendu transparent avec des sinus frontaux découpés en noir. Crania a évolué à peu près à la même taille afin de montrer la taille relative des sinus frontaux à crania, les barres d'échelle sous crania = 1cm. Détail de l'insert de sinus frontal de Ceprano qualitativement différent, montré de l'aspectus superialis. À l'exception de Ceprano, les sinus frontaux des quatre échantillons sont uniques et continus.

Figure 8: A comparison of maxillary sinuses between species. Virtual reconstructions of crania showing sectioned out maxillary sinuses rendered in black in (Top to bottom) Petralona (*H. heidelbergensis*), Guattari (*H. neanderthalensis*) and a recent *H. sapiens* from Mexico. Left view: norma frontalis, right view: norma lateralis. The norma lateralis view for Petralona is flipped horizontally for consistency and ease of comparison, since only the left maxillary sinus is fully preserved in this fossil. Crania scaled to approximately the same size in order to show relative size of maxillary sinuses, scale bars under crania = 1cm.

French Figure 8: Une comparaison des sinus maxillaires entre les espèces. Reconstructions virtuelles de crâne montrant des sinus maxillaires sectionnés en noir dans (de haut en bas)

Petralona (*H. heidelbergensis*), Guattari (*H. neanderthalensis*) et un récent *H. sapiens* du Mexique. Vue de gauche: norma frontalis, vue de droite: norma lateralis. La vue de Norma lateralis pour Petralona est inversée horizontalement pour la cohérence et la facilité de comparaison, puisque seulement le sinus maxillaire gauche est entièrement préservé dans ce fossile. Crania a mis à l'échelle à peu près la même taille afin de montrer la taille relative des sinus maxillaires, les barres d'échelle sous crania = 1cm.

Tables

Specimen/Group	Taxonomic group	Geographic location	Date	Number in sample	Medical/ microCT	Source	FVS Y/N (sample n where >1)	FSS Y/N (sample n where >1)	MVS Y/N (sample n where >1)	MSS Y/N (sample n where >1)
KNM-ER 3883	*H. erectus*	Kenya	1.5-6 Ma [95]	1	Medical	KNM	N	N	N	N
Steinheim	*H. heidelbergensis*	Germany	>300 ka, MIS 9 [96]	1	Medical	UV	N	Y	N	N
Broken Hill	*H. heidelbergensis*	Zambia	~250-300 ka [97]	1	Medical	NHM	Y	Y	Y	Y
Bodo	*H. heidelbergensis*	Ethiopia	~600 ka [81]	1	Medical	UV	Y	N	Y	N
Petralona	*H. heidelbergensis*	Greece	~400 ka [75]	1	Medical	UV/UT	Y	Y	Y	Y
Ceprano	*H. heidelbergensis*	Italy	430-385 ka [98]	1	Medical	ULS	Y	N	N	N
Guattari	*H. neanderthalensis*	Italy	57-51 ka [99]	1	Medical	MNPE	Y	N	Y	N
Krapina 3	*H. neanderthalensis*	Croatia	~130 ka [100]	1	Medical	NESPOS	Y	N	N	N
Tabun C1	*H. neanderthalensis*	Israel	~122 ka [101]	1	Medical	NHM	Y	N	N	N
Forbes' Quarry	*H. neanderthalensis*	Gibraltar	~ 50 ka [102]	1	Medical	NHM	Y	N	Y	N
La Chapelle-aux-Saints 1	*H. neanderthalensis*	France	~ 50 ka [103]	1	Medical	MH	Y	Y	Y	Y
La Ferrassie 1	*H. neanderthalensis*	France	75 – 60 ka [104]	1	Medical	MH	Y	Y	Y	Y
La Quina 5	*H. neanderthalensis*	France	75-48 ka [104], [105]	1	Medical	MH	Y	N	N	N
Feldhofer Neanderthal	*H. neanderthalensis*	Germany	~40 ka [106]	1	Medical	UZ	Y	N	N	N
Skhul 5	Early *H. sapiens*	Israel	130-100 ka [107]	1	Medical	NESPOS	Y	N	N	N
Singa	Early *H. sapiens*	Sudan	>131-135 ka [103]	1	micro	NHM	Y	N	N	N

Mladeč 1	Early *H. sapiens*	Czech Republic	~37.5-34.75 ka [108]	1	Medical	UV	Y	N	Y	Y
Cro-Magnon 1	Early *H. sapiens*	France	<28 ka [109]	1	Medical	MH	Y	N	Y	N
Cro-Magnon 2	Early *H. sapiens*	France	<28 Ka [109]	1	Medical	MH	Y	Y	N	N
Cro-Magnon 3	Early *H. sapiens*	France	<28 Ka [109]	1	Medical	MH	Y	N	N	N
Ngaloba	Early *H. sapiens*	Tanzania	50-120 ka [110], [111]	1	Medical	UV	Y	N	N	N
Lithuania	Recent *H. sapiens*	Lithuania	<25 ka	14	Medical	TK	Y (11)	Y (10)	Y (11	Y (8)
Western Africa	Recent *H. sapiens*	Angola, Liberia, Nigeria	<25 ka	13	Medical	ORSA	Y (13)	Y (8)	Y (12)	Y (8)
Western Europe	Recent *H. sapiens*	Germany, The Netherlands, Norway, Sweden	<25 ka	12	Medical	NESPOS	Y (11)	Y (10)	Y (10)	Y (10)
India	Recent *H. sapiens*	India	<25 ka	12	Medical	ORSA	Y (11)	Y (10)	Y (10)	Y (5)
Greenland	Recent *H. sapiens*	Greenland	<25 ka	7	micro	NHM	Y (7)	Y (7)	Y (7)	Y (7)
Russia	Recent *H. sapiens*	Russia	<25 ka	4	Medical	ORSA	Y (4)	Y (4)	Y (4)	Y (2)
North Africa	Recent *H. sapiens*	Algeria, Morocco	<25 ka	7	Medical	IPH	Y (7)	Y (3)	Y (2)	Y (1)
Tasmania	Recent *H. sapiens*	Tasmania	<25 ka	8	micro	NHM	Y (8)	Y (5)	Y (8)	Y (3)
Torres Straits Islands	Recent *H. sapiens*	Torres Straits Islands	<25 ka	15	micro	NHM	Y (12)	Y (10)	Y (12)	Y (8)

Peru	Recent *H. sapiens*	Peru	<25 ka	10	Medical	ORSA	Y (10)	Y (10)	Y (10)	Y (10)
China	Recent *H. sapiens*	China	<25 ka	10	Medical	ORSA	Y (9)	Y (9)	Y (10)	Y (8)
Hawaii	Recent *H. sapiens*	Hawaii	<25 ka	11	micro	NHM	Y (11)	Y (10)	Y (10)	Y (8)
Mexico	Recent *H. sapiens*	Mexico	<25 ka	10	Medical	ORSA	Y (10)	Y (8)	Y (9)	Y (5)

154

Replication	Frontal	Maxillary
1	7616.8	17214.2
2	7785.7	16947.0
3	7353.4	16688.7
4	7598.5	16735.8
5	7751.4	18416.8
Mean	**7621.2**	**17200.5**
Standard deviation	**170.5**	**710.9**
% error	**1.8**	**2.9**

1155
1156

Landmark	Definition	Number in frontal sinus-specific landmark set
Bregma	Point where coronal & sagittal sutures intersect	1
Glabella	Most anterior point on frontal bone	2
Nasion	Point of intersection of nasofrontal suture & midsagittal plane	3
C/P3	Most inferior external point between maxillary canine (C) and first pre-molar (P3)	4
Frontomalare orbitale	Point where zygomaticofrontal suture crosses orbital margin	5
Zygoorbitale	Point where zygomaticomaxillary suture intersects with inferior orbital margin	6
Frontotemporale	Point on frontal bone where temporal line reaches its most anteromedial position	7
Frontomalare temporale	Most lateral point on zygomaticofrontal suture	8
Porion	Most superior point on margin of external auditory meatus	9
Lambda	Point where sagittal & lambdoid sutures intersect	10

Landmark	Definitions	Number in maxillary sinus-specific landmark set
Bregma	Point where coronal & sagittal sutures intersect	1
Glabella	Most anterior point on frontal bone	2
Nasion	Point of intersection of nasofrontal suture & midsagittal plane	3
Alare	Most lateral point on nasal aperture taken perpendicular to nasal height	4
C/P3	Most inferior external point between maxillary canine (C) and first pre-molar (P3)	5
Zygoorbitale	Point where zygomaticomaxillary suture intersects with inferior orbital margin	6
Zygion	Most lateral point on surface of zygomatic arch	7
Zygomaxillare	Most inferoanterior point on zygomaticomaxillary suture	8
Molars pos.	Most inferoposterior point on external maxillary alveolus (posterior to M3)	9
Porion	Most superior point on margin of external auditory meatus	10
Lambda	Point where sagittal & lambdoid sutures intersect	11
Ectomolare	Most lateral point on outer surface of alveolar margin of maxilla	12
Orale	Point of intersection on palate with line tangent to posterior margins of central incisor alveoli	13

Landmark set	PC	Variance explained (%)	Direction of relationship	r^2	p	Bonferroni correction
Frontal sinus-specific	6	7	Negative	0.12	< 0.001	Yes
Maxillary sinus-specific	3	11	Positive	0.41	< 0.001	Yes

	H. sapiens	*H. neanderthalensis*	*H. heidelbergensis*
H. sapiens		0.05848	**0.6914***
H. neanderthalensis	1		**0.6930***
H. heidelbergensis	**0.0006***	**0.0186***	

1163
1164

	H. sapiens	*H. neanderthalensis*	*H. heidelbergensis*
H. sapiens		**0.6059***	**0.4542***
H. neanderthalensis	**0.0001***		-0.0714
H. heidelbergensis	**0.0147***	0.5275	

1165
1166

	H. sapiens	*H. neanderthalensis*	*H. heidelbergensis*
H. sapiens		0.311	**0.591***
H. neanderthalensis	0.194		-0.25
H. heidelbergensis	**0.015***	1	

	H. sapiens	*H. neanderthalensis*	*H. heidelbergensis*
H. sapiens		**0.9599***	**0.6119***
H. neanderthalensis	**0.0001***		1
H. heidelbergensis	**0.0062***	0.3447	

Figures

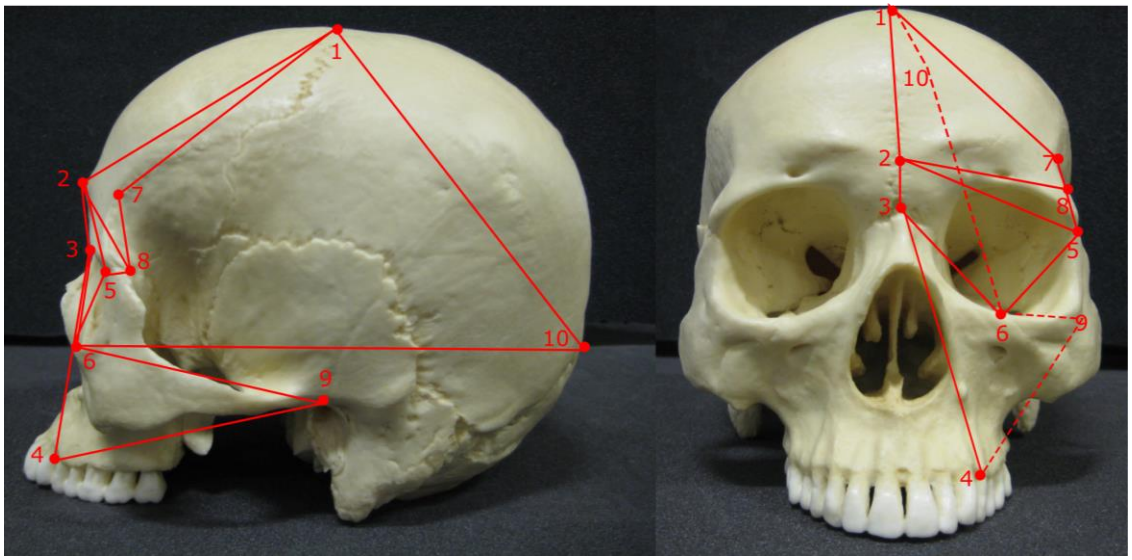
1
2
7
3
8
5
10
6
9
4
1
10
2
7
3
8
5
6
9
4

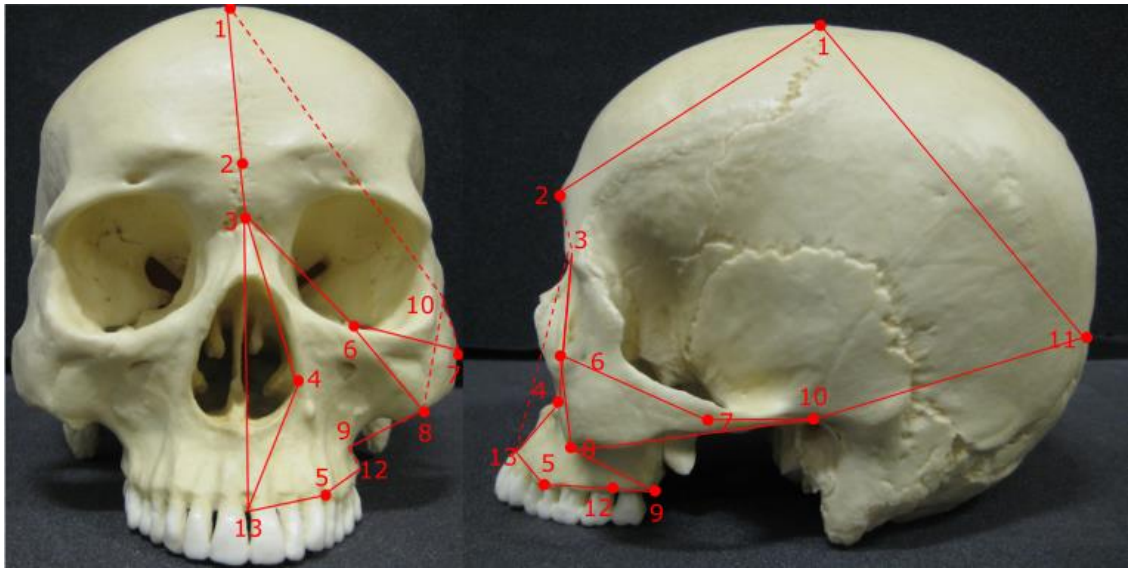
1
2
3
10
6
7
4
9
8
5
12
13
1
2
3
11
6
4
10
7
8
13
5
12
9

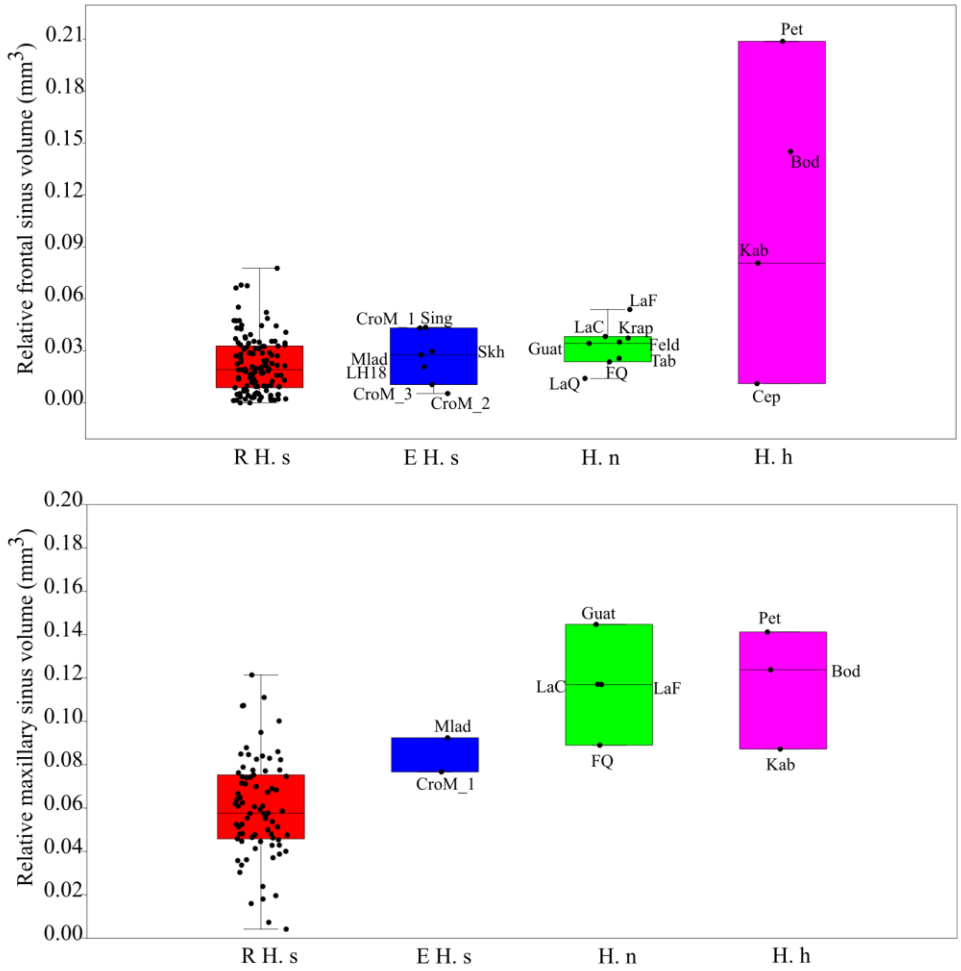

1179
1180
1181

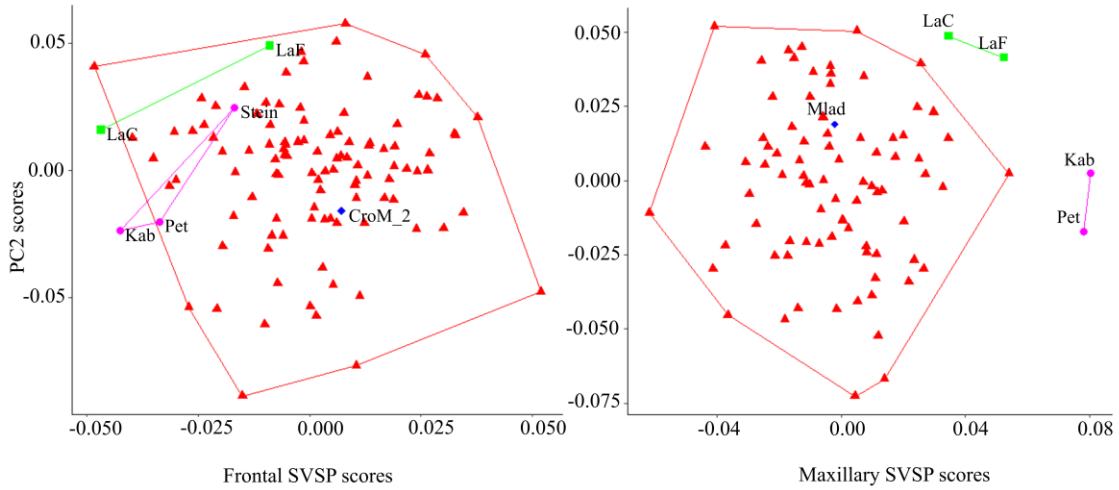

1182
1183
1184

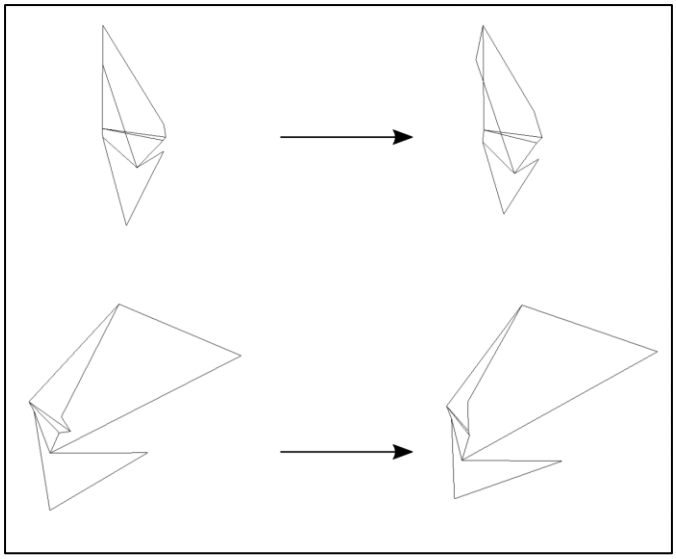

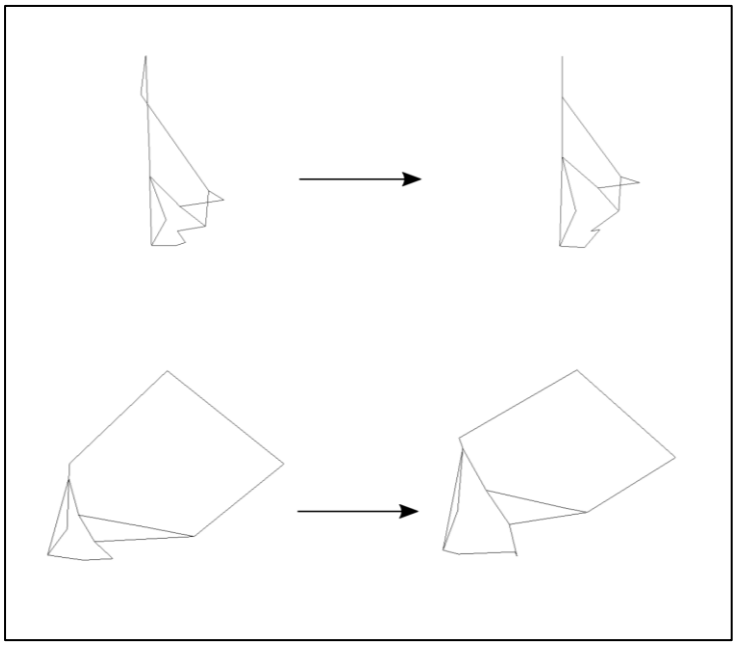

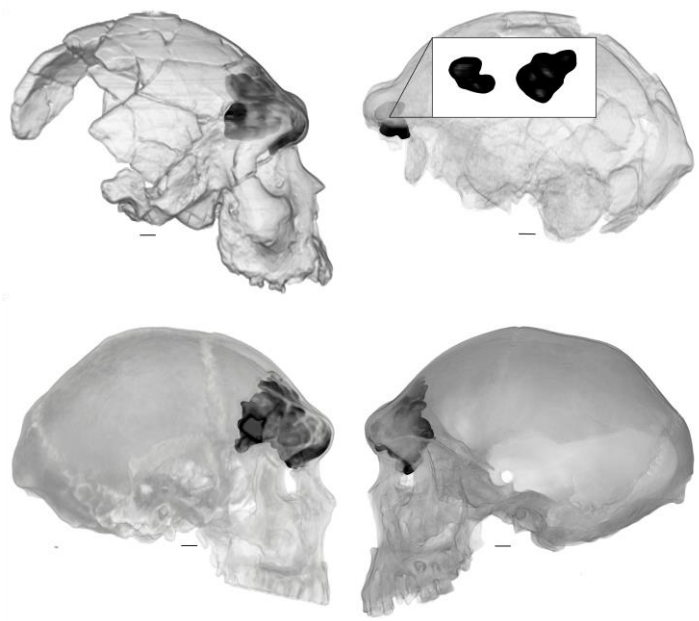

1191
1192
1193

1194